

Reduced-order models for flow control

Clancy Rowley

17 October 2008

7th ERCOFTAC SIG33 - FLUBIO workshop on
Open issues in transition and flow control
Santa Margherita Ligure, Italy

Mechanical
and Aerospace
Engineering

PRINCETON



Acknowledgements

- Acknowledgments

- Students

Milos Ilak
(channel flow)



Sunil Ahuja
(airfoil separation)



- Postdoc

- Mingjun Wei (NMSU)
(free shear flow)



- Collaborators

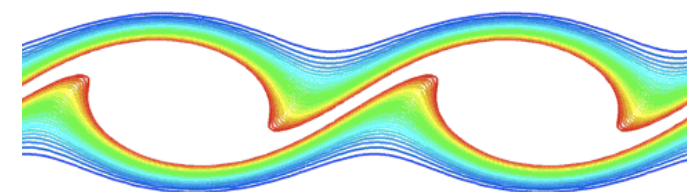
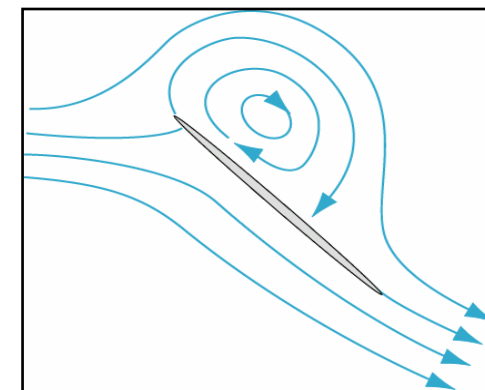
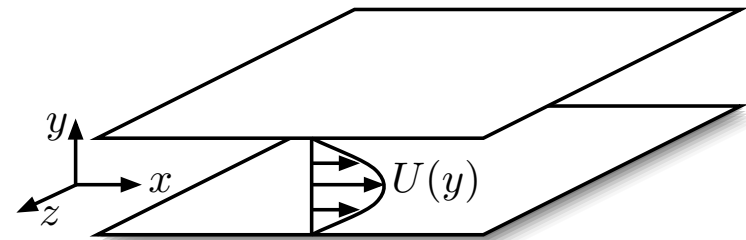
- Yannis Kevrekidis (Princeton)
 - Dave Williams (IIT)
 - Tim Colonius, Sam Taira (Caltech)
 - Gilead Tadmor (Northeastern)

- Funding from NSF and AFOSR



Outline

- Reduced-order models: POD and balanced truncation
 - Importance of inner product for Galerkin projection
 - Balanced truncation
 - Method of snapshots
- Applications
 - Linearized channel flow
 - Separating flow past an airfoil
- Dynamically scaling POD modes
 - Free shear layer
 - Scaled basis functions
 - Template fitting
 - Equations for the shear layer thickness

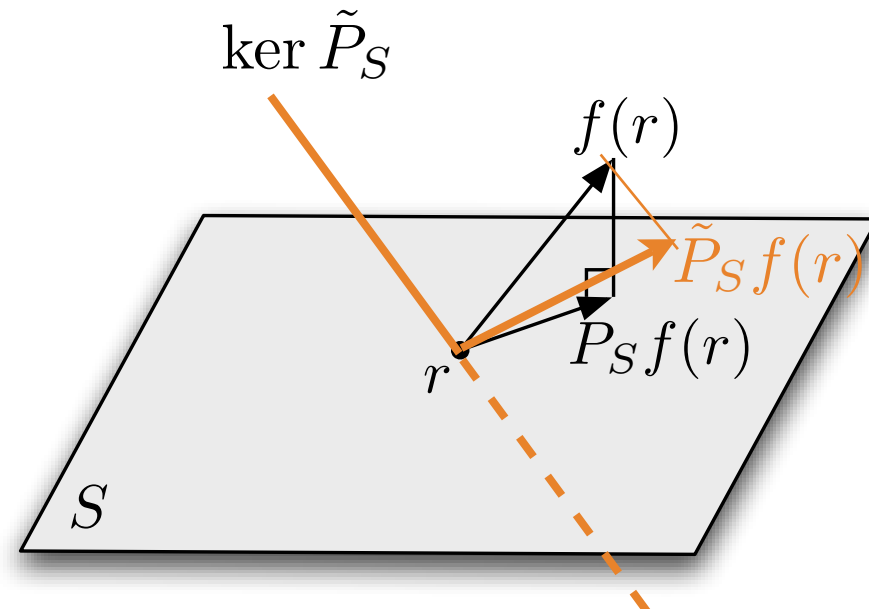


Galerkin projection

- Dynamics evolve on a high-dimensional space (or infinite-dim'l)
- Project dynamics onto a low-dimensional subspace S

$$\dot{x} = f(x) \quad x \in V$$

$$r \in S \subset V$$



- Define dynamics on the subspace by

$$\dot{r} = P_S f(r) \quad P_S : V \rightarrow S \text{ is a projection}$$

- Two choices:
 - choice of subspace
 - choice of inner product
(equivalently, choice of the nullspace for a non-orthogonal projection)



Proper Orthogonal Decomposition (POD)

- Obtain “optimal” basis for the subspace, from data
 - Gather data, as “snapshots” $u(x,t)$ from simulations or experiments
 - Determine orthonormal basis functions that optimally span the data:

$$P_n u(x, t) = \sum_{j=1}^n a_j(t) \varphi_j(x)$$

- Minimize $\int_0^T \|u(t) - P_n u(t)\|^2 dt$

- Solution: SVD of the matrix of snapshots

- Limitations

- Optimal for capturing a given dataset, not necessarily dynamics
- Low-energy modes may be important to the dynamics
- POD says nothing about which inner product you should use

$$\begin{aligned} \varphi_j &\in V \\ &\text{POD modes} \\ S &= \text{span}\{\varphi_j\} \end{aligned}$$



Energy-based inner products

- Reduced-order models can behave unpredictably
 - Can even change stability type of equilibria!
[Rempfer, Thoret. CFD 2000]
- Energy-based inner products behave better
 - Consider a system with a stable equilibrium point at the origin
 - An **energy-based** inner product induces a norm that is a Liapunov function:

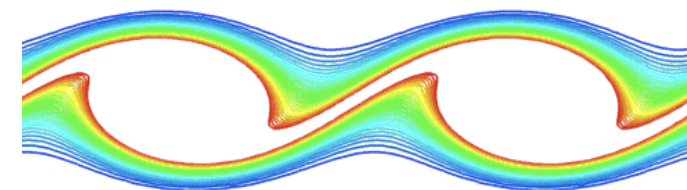
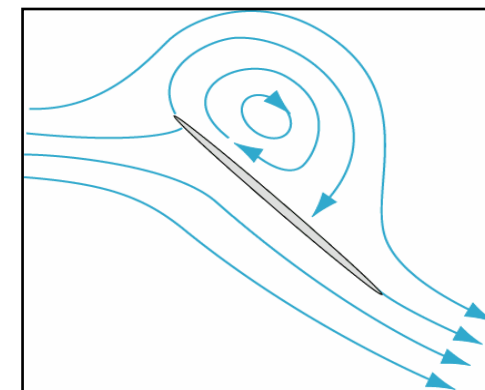
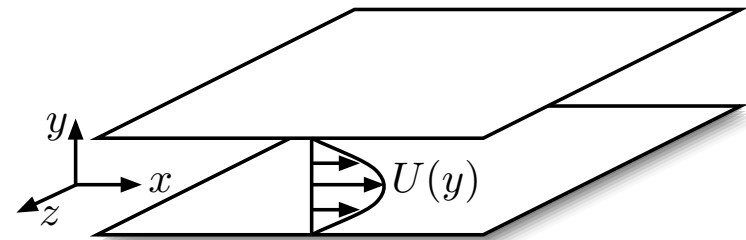
$$\langle x, y \rangle = x^T Q y, \quad Q > 0 \quad \begin{array}{l} V(x) = x^T Q x \text{ is a Liapunov function} \\ \dot{V}(x) = 2x^T f(x) \leq 0, \quad \forall x \in U \end{array}$$

- Useful result: if such an inner product is used for Galerkin projection, the reduced-order model is guaranteed to have the same stability type as the full system [Rowley, Colonius, Murray, Phys D 2004]
- One interpretation of balanced truncation: use adjoint simulations to determine an appropriate inner product (the “observability Gramian,” always a Lyapunov function)



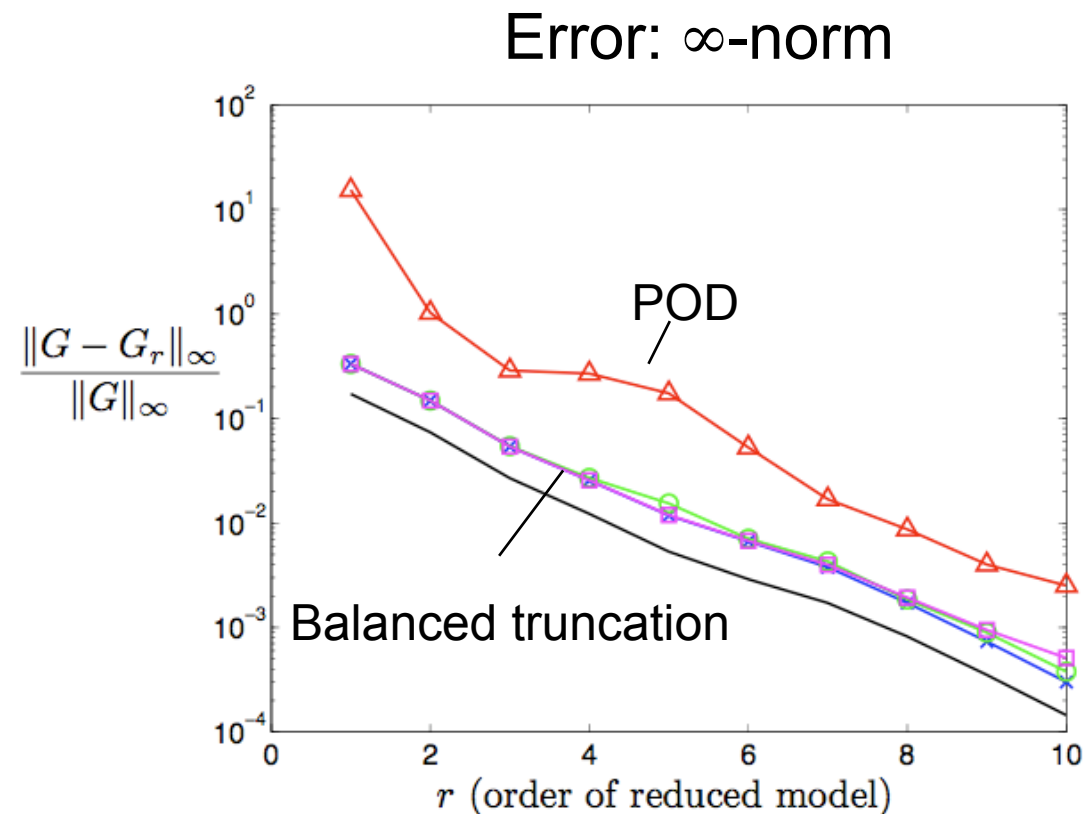
Outline

- Reduced-order models: POD and balanced truncation
 - Importance of inner product for Galerkin projection
 - Balanced truncation
 - Method of snapshots
- Applications
 - Linearized channel flow
 - Separating flow past an airfoil
- Dynamically scaling POD modes
 - Free shear layer
 - Scaled basis functions
 - Template fitting
 - Equations for the shear layer thickness



Are POD modes optimal?

- POD modes are not optimal for Galerkin projection
 - POD determines a subspace that optimally captures the **energy** in a given dataset
 - These modes are usually **not optimal** for Galerkin projection
 - **Low-energy modes** can play an important role in the dynamics [Aubry, Holmes, Lumley, 1988; Smith 2002 PhD thesis, Princeton]
 - Can often do better with **balanced truncation** [Moore 1981]



Balanced truncation

- Why doesn't everybody use this?
 - Valid for stable, linear systems
 - Extensions for unstable systems [Jonckheere & Silverman 1983, Zhou 2001]
 - Extensions for nonlinear systems [Scherpen 1993, Lall, Marsden, Glavaski 1999]
 - Computationally expensive for large systems
 - n^3 computational time: $n > 10^5$ for typical fluids simulations
- Improvements for large systems
 - POD is tractable for large systems. Can we extend, e.g., the **method of snapshots**, to compute balancing transformations?
 - Based on earlier snapshot-based methods:
 - Lall, Marsden, & Glavaski, 1999
 - Willcox & Peraire, 2001



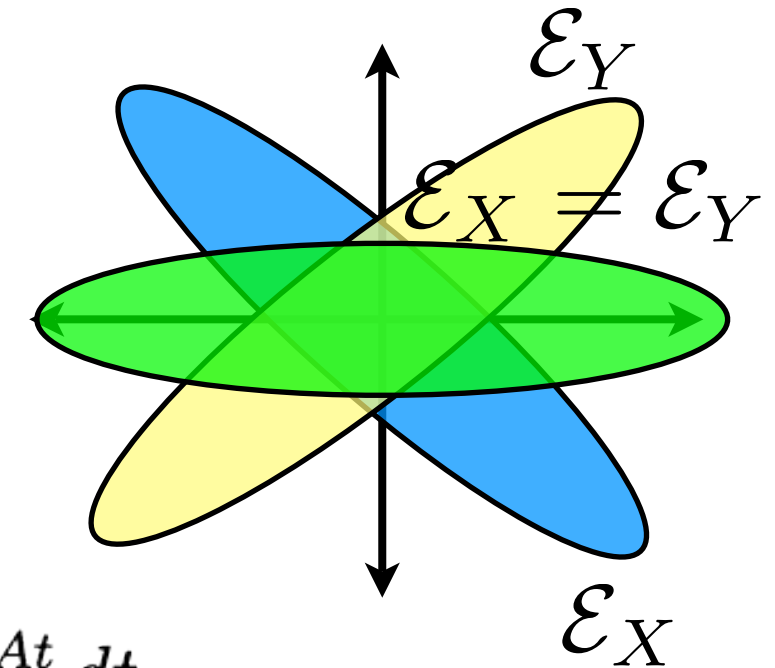
Overview of balanced truncation

- Start with a stable, linear input-output system

$$\dot{x} = Ax + Bu$$

$$y = Cx$$

What are you interested in capturing?



- Compute controllability and observability Gramians

$$X = \int_0^{\infty} e^{At} BB^* e^{A^*t} dt$$

$$AX + XA^* + BB^* = 0$$

$$Y = \int_0^{\infty} e^{A^*t} C^* C e^{At} dt$$

$$A^*Y + YA + C^*C = 0$$

States easily excited
by an input

States that have large influence
on the output

- Find a transformation T that simultaneously diagonalizes X and Y

$$x = Tz, \quad T^{-1}X(T^{-1})^* = T^*YT = \Sigma = \begin{bmatrix} \sigma_1 & & \\ & \ddots & \\ & & \sigma_n \end{bmatrix}$$

- Change coordinates, and truncate states that are least controllable/observable



Empirical Gramians

- Construct Gramians from impulse response data

- Not solving Liapunov equations
- For a single input: compute impulse-state response:

$$\begin{aligned} \dot{x} &= Ax, & x(0) &= B \\ \text{solution} & & x(t) &= e^{At} B \end{aligned}$$

- The controllability Gramian is then $W_c = \int_0^{\infty} x(t)x(t)^T dt$

- Discretize in time, collect snapshots into a matrix:

$$X = \begin{bmatrix} | & & | \\ x(t_1) & \cdots & x(t_m) \\ | & & | \end{bmatrix}$$

- Then $W_c \approx XX^T$
- For observability Gramian, same procedure, but use adjoint equations $\dot{z} = A^* z \quad z(0) = C^*$

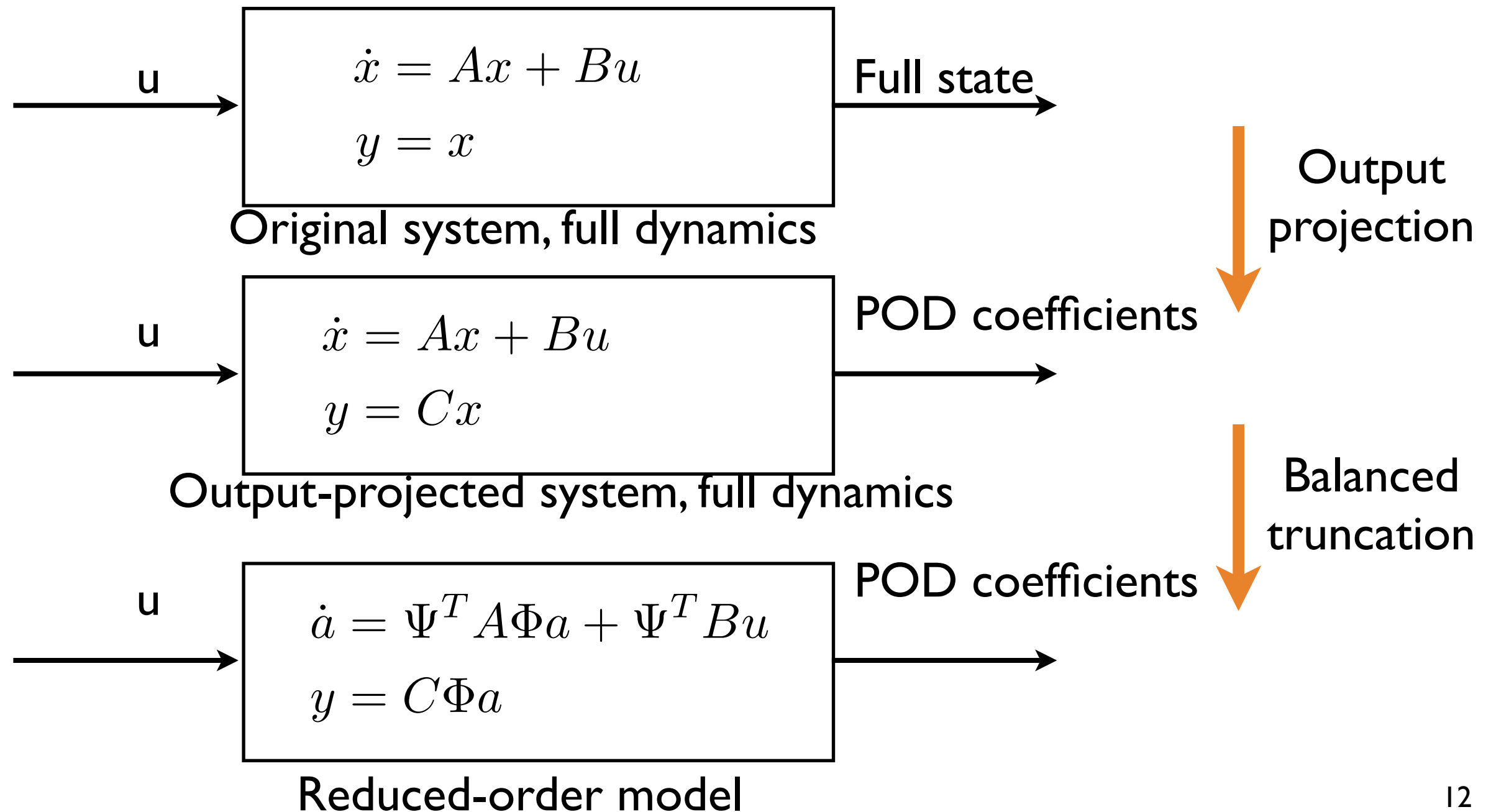
- For multiple inputs/outputs, same procedure, but do one impulse-response for each input/output

[Lall et al, 1999]



Large numbers of outputs

- Often, we are interested in modeling the full state
 - If dimension is large, project output onto POD modes
 - POD gives optimally-close output-projected system (in 2-norm)



Approximate balanced truncation for large systems

- Method of snapshots enables one to compute approximate balanced truncations with cost similar to POD
 - One simulation for each control input, one adjoint simulation for each output
 - One SVD, (# direct snapshots) \times (# adjoint snapshots)
 - If number of outputs is large, method for projection onto smaller-rank output
- Balanced truncation is just POD with respect to an inner product defined by the observability Gramian Y :

$$\langle x_1, x_2 \rangle_Y = x_1^T Y x_2$$

- Observability Gramian is always a Liapunov function \Rightarrow preserves stability!
- Obtain set of bi-orthogonal modes:

direct modes: $\{\varphi_1, \dots, \varphi_n\}$

adjoint modes: $\{\psi_1, \dots, \psi_n\}$

bi-orthogonal: $\langle \psi_i, \varphi_j \rangle = \delta_{ij}$

Galerkin:

$$\dot{x} = f(x)$$

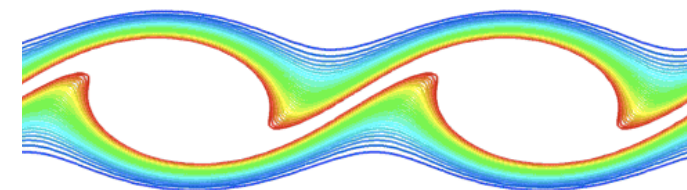
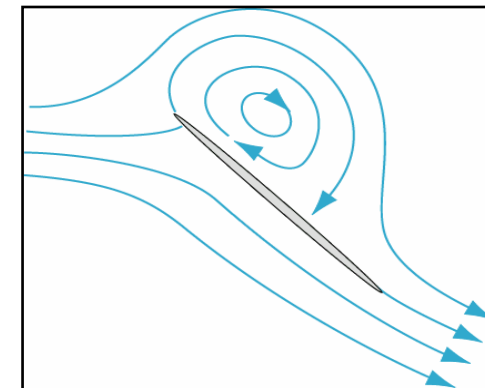
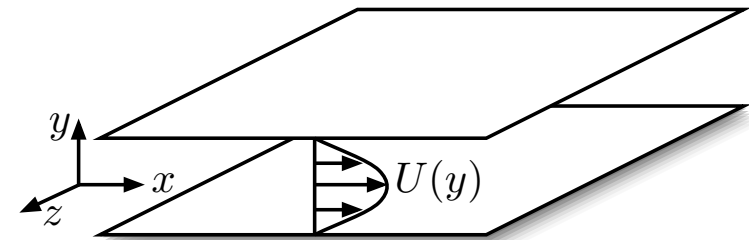
$$x(t) = \sum_j a_j(t) \varphi_j$$

$$\dot{a}_j(t) = \langle \psi_j, f(x) \rangle$$



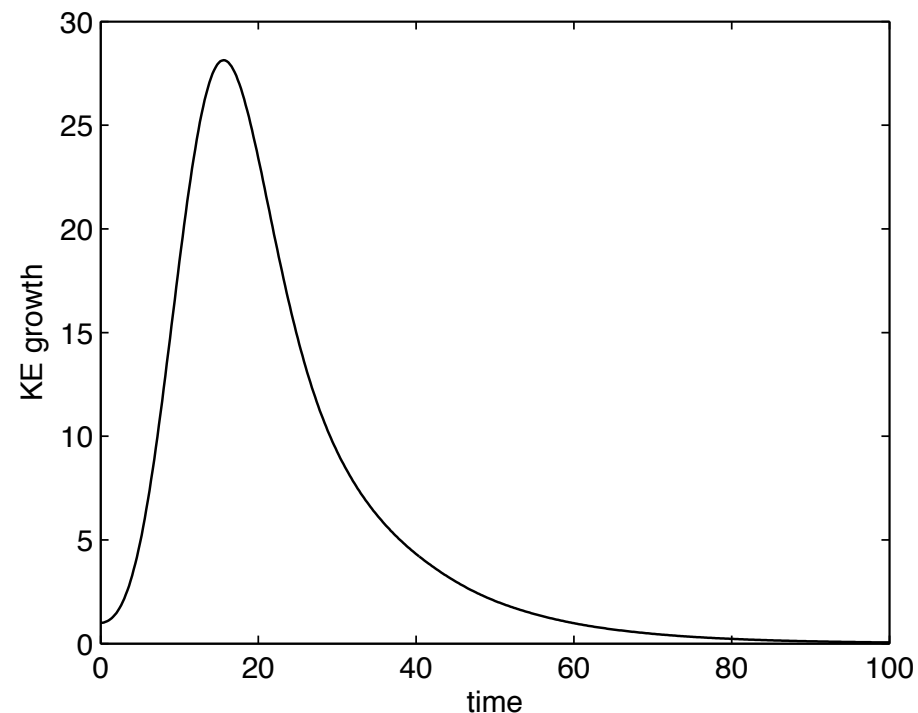
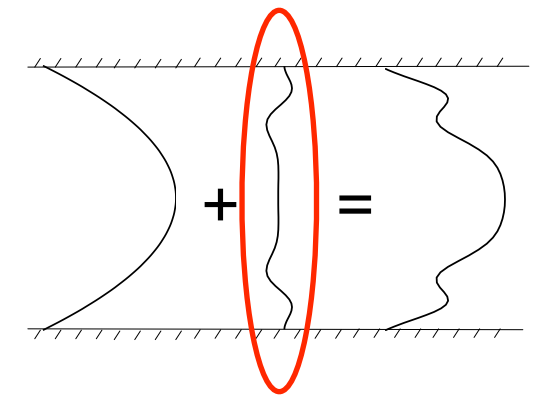
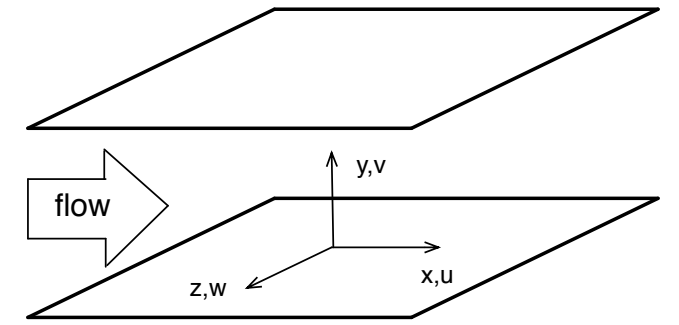
Outline

- Reduced-order models: POD and balanced truncation
 - Importance of inner product for Galerkin projection
 - Balanced truncation
 - Method of snapshots
- Applications
 - Linearized channel flow
 - Separating flow past an airfoil
- Dynamically scaling POD modes
 - Free shear layer
 - Scaled basis functions
 - Template fitting
 - Equations for the shear layer thickness



Application: Linearized Channel Flow

- Plane channel flow with periodic boundary conditions
 - Goal: delay transition to turbulence using feedback control
 - Goal: improved understanding of transition mechanisms
 - Focus: low-dimensional models of transition
- Linear development of small perturbations
 - Transition not predicted correctly by linear stability theory
 - Non-normality of the governing operator results in large transient growth, even though linearized flow is stable
 - Large linear system with complex dynamic behavior



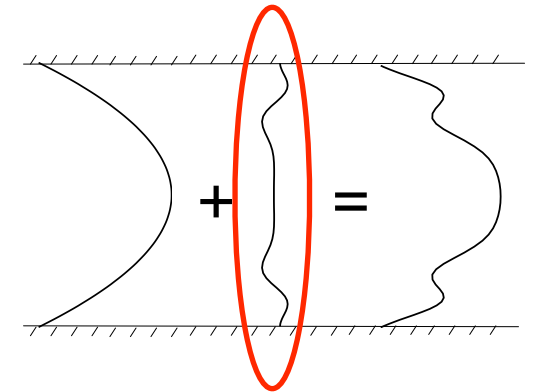
Previous work:

Trefethen et al [Science, 1993]
Farrell & Ioannou [96,96,01]
Schmid & Henningson [01]
Bamieh & Jovanovic [01,03]



Governing Equations

- Navier-Stokes equations linearized about a laminar profile
- Perturbation dynamics fully described by wall-normal velocity v and wall-normal vorticity η
- Clamped boundary conditions $v(\pm 1) = \frac{\partial v}{\partial y}(\pm 1) = 0$



Orr-Sommerfeld/Squire system	Adjoint system
$\frac{\partial}{\partial t} \begin{bmatrix} -\Delta & 0 \\ 0 & I \end{bmatrix} \begin{bmatrix} v \\ \eta \end{bmatrix} = \begin{bmatrix} L_{OS} & 0 \\ -U' \partial_z & L_{SQ} \end{bmatrix} \begin{bmatrix} v \\ \eta \end{bmatrix}$	$\frac{\partial}{\partial t} \begin{bmatrix} -\Delta & 0 \\ 0 & I \end{bmatrix} \begin{bmatrix} v \\ \eta \end{bmatrix} = \begin{bmatrix} L_{OS}^* & U' \partial_z \\ 0 & L_{SQ}^* \end{bmatrix} \begin{bmatrix} v \\ \eta \end{bmatrix}$
$L_{OS} = U \partial_x \Delta - U'' \partial_x - \frac{1}{Re} \Delta^2$	$L_{OS}^* = -U \partial_x \Delta - 2U' \partial_x \partial_y - \frac{1}{Re} \Delta^2$
$L_{SQ} = -U \partial_x + \frac{1}{Re} \Delta$	$L_{SQ}^* = U \partial_x + \frac{1}{Re} \Delta$

$$\dot{x} = Ax + \underbrace{Bu_1}_{\text{actuation}} + \underbrace{Fu_2}_{\text{disturbances}}$$

- System in standard state-space form with actuation and disturbances

Analysis as an input-output system: Bamieh & Jovanovic [01,03]

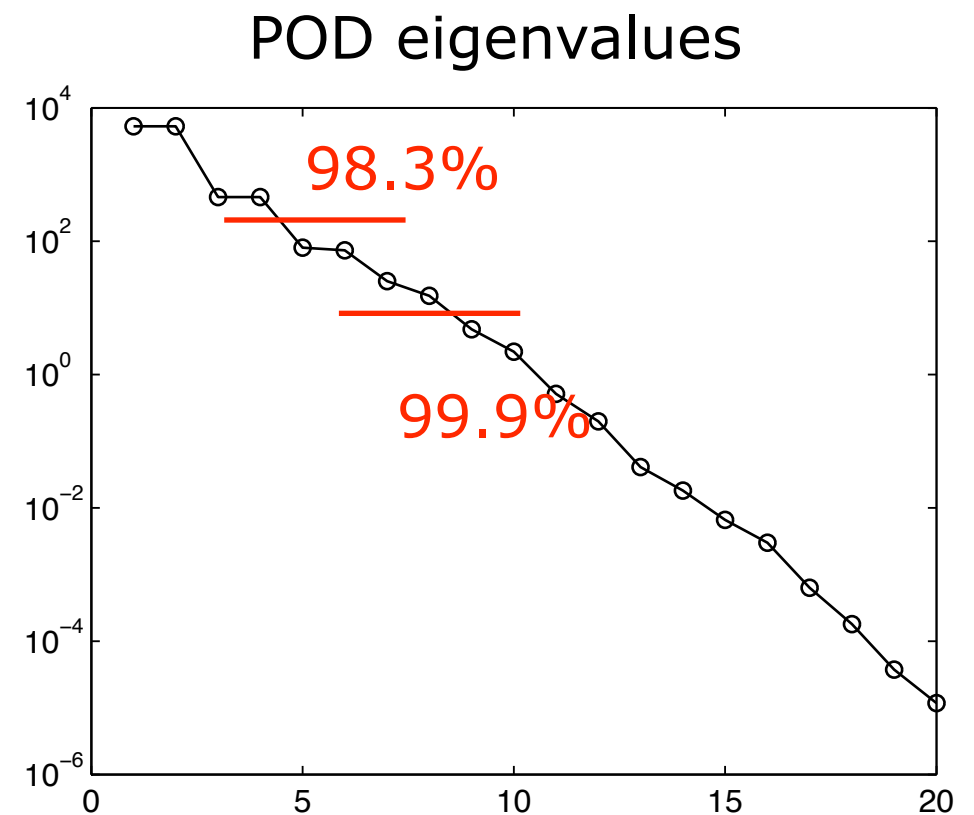
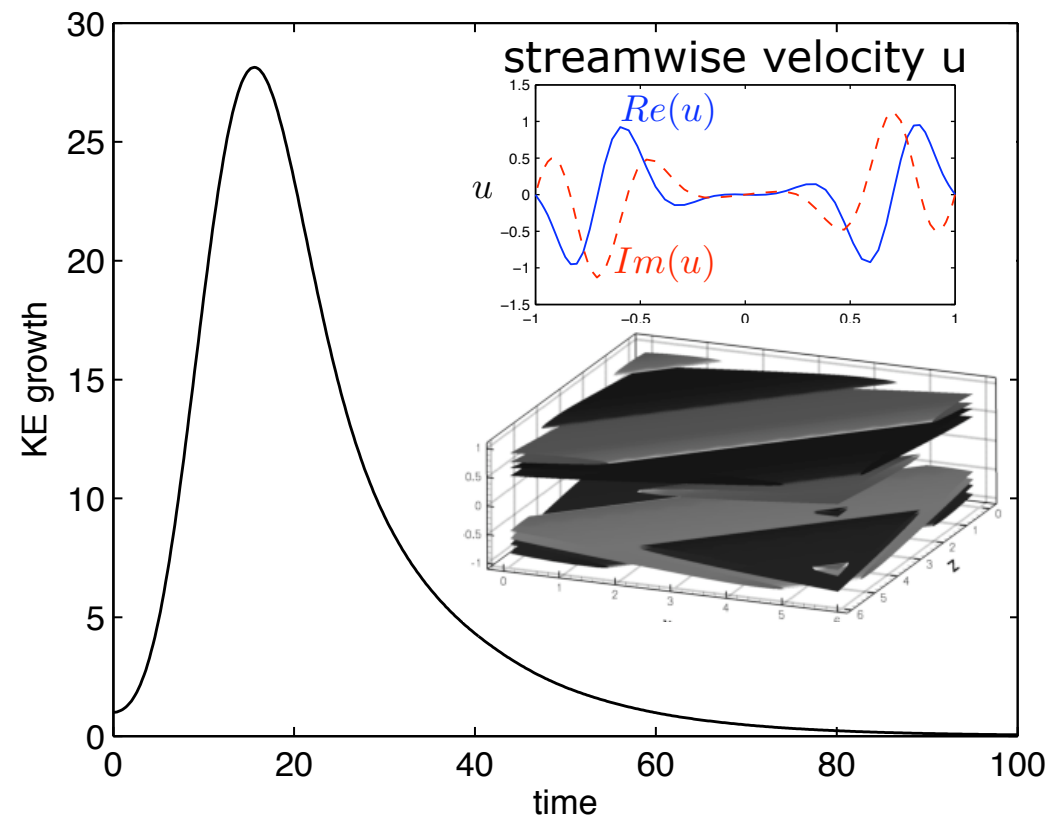


Single-wavenumber perturbation - optimal

- Perturbations of the form

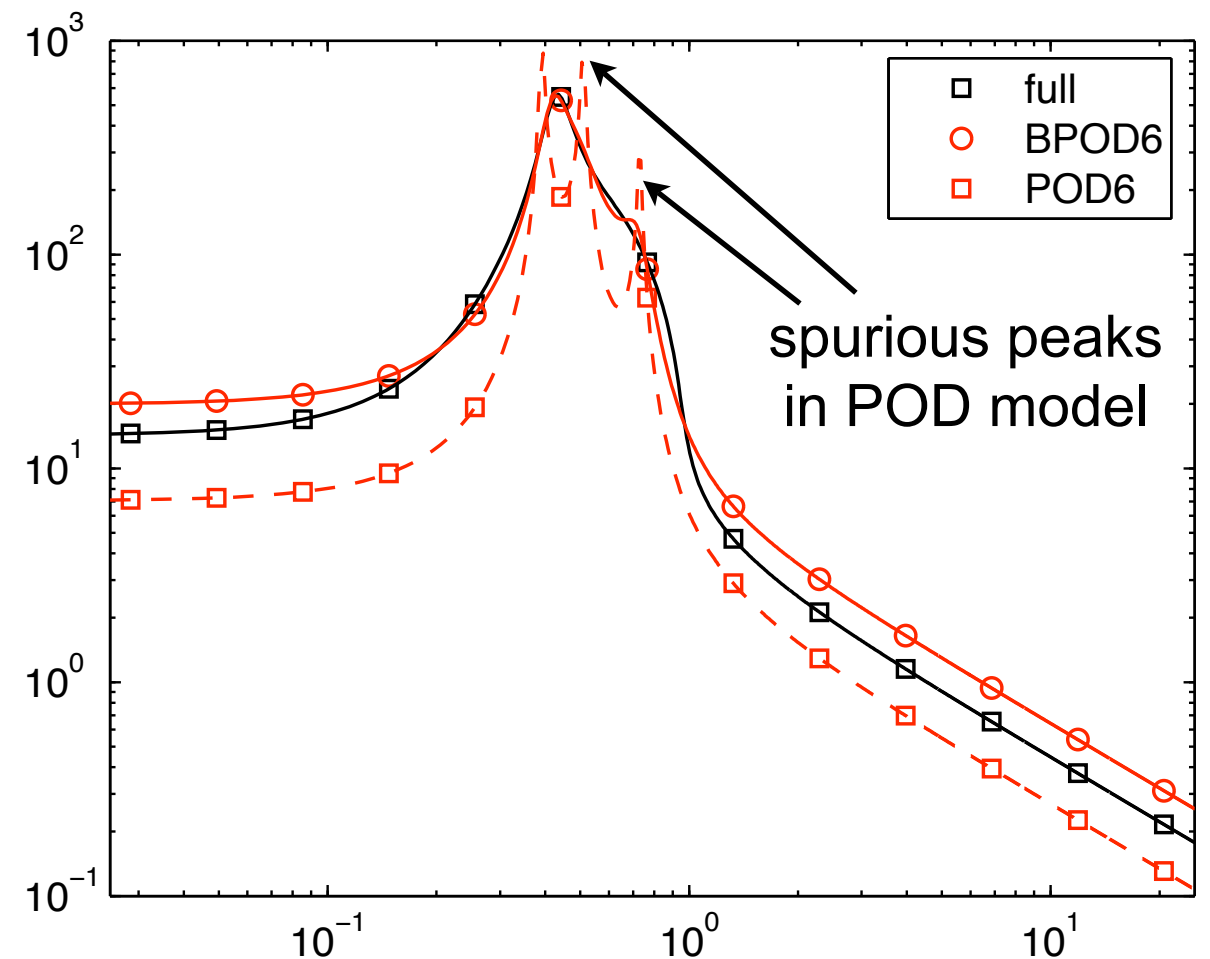
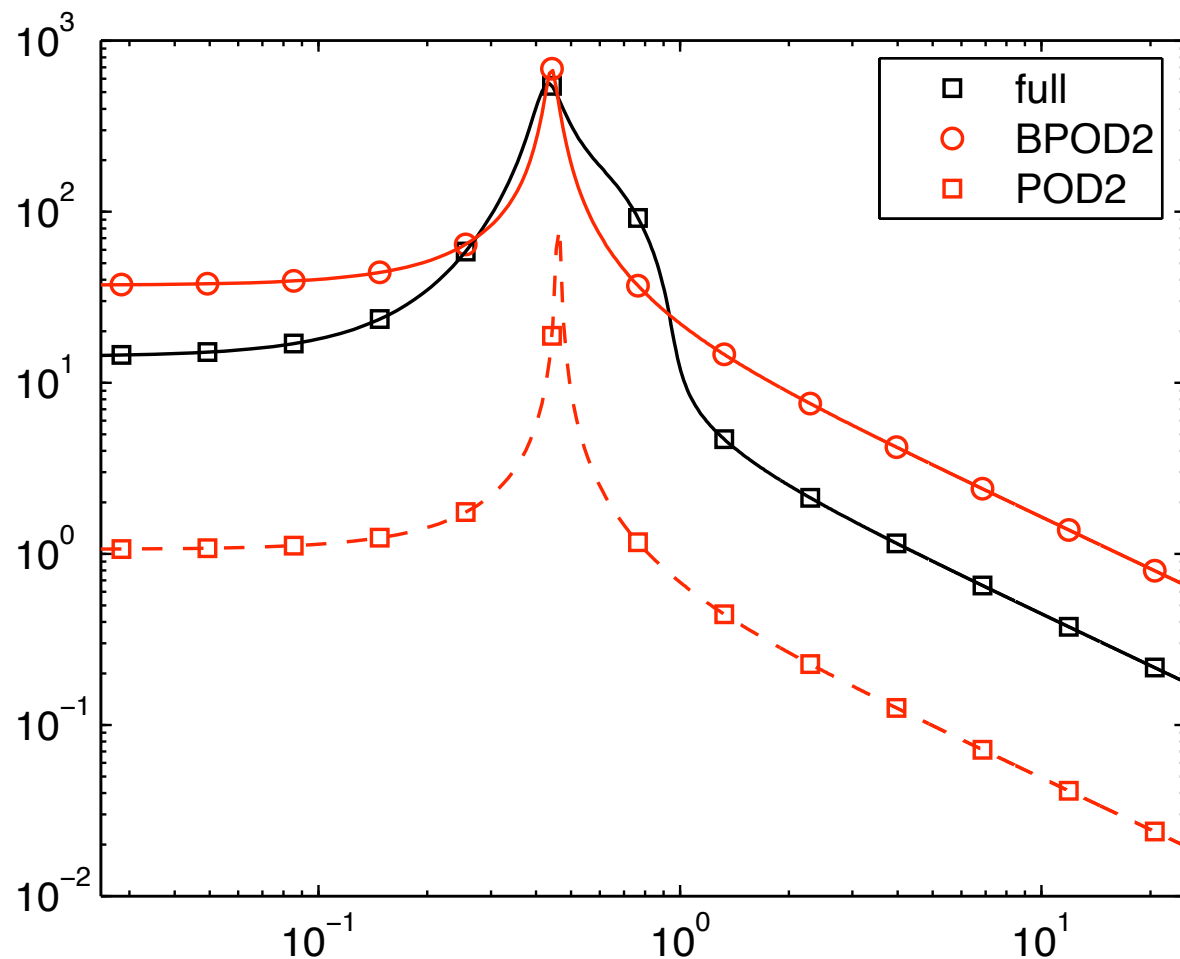
$$q = \hat{q}(y)e^{i\alpha x + i\beta z + \lambda t} \quad q = \begin{bmatrix} v \\ \eta \end{bmatrix}$$

- System can be analyzed in 1-D so that full balanced truncation is tractable, allowing comparison with the BPOD approximation and POD
- Well-studied cases (Farrell, Henningson, Reddy, Schmid, Jovanovic, Bamieh)
- Case presented here $\alpha=1$, $\beta=1$ and exhibits rich dynamics



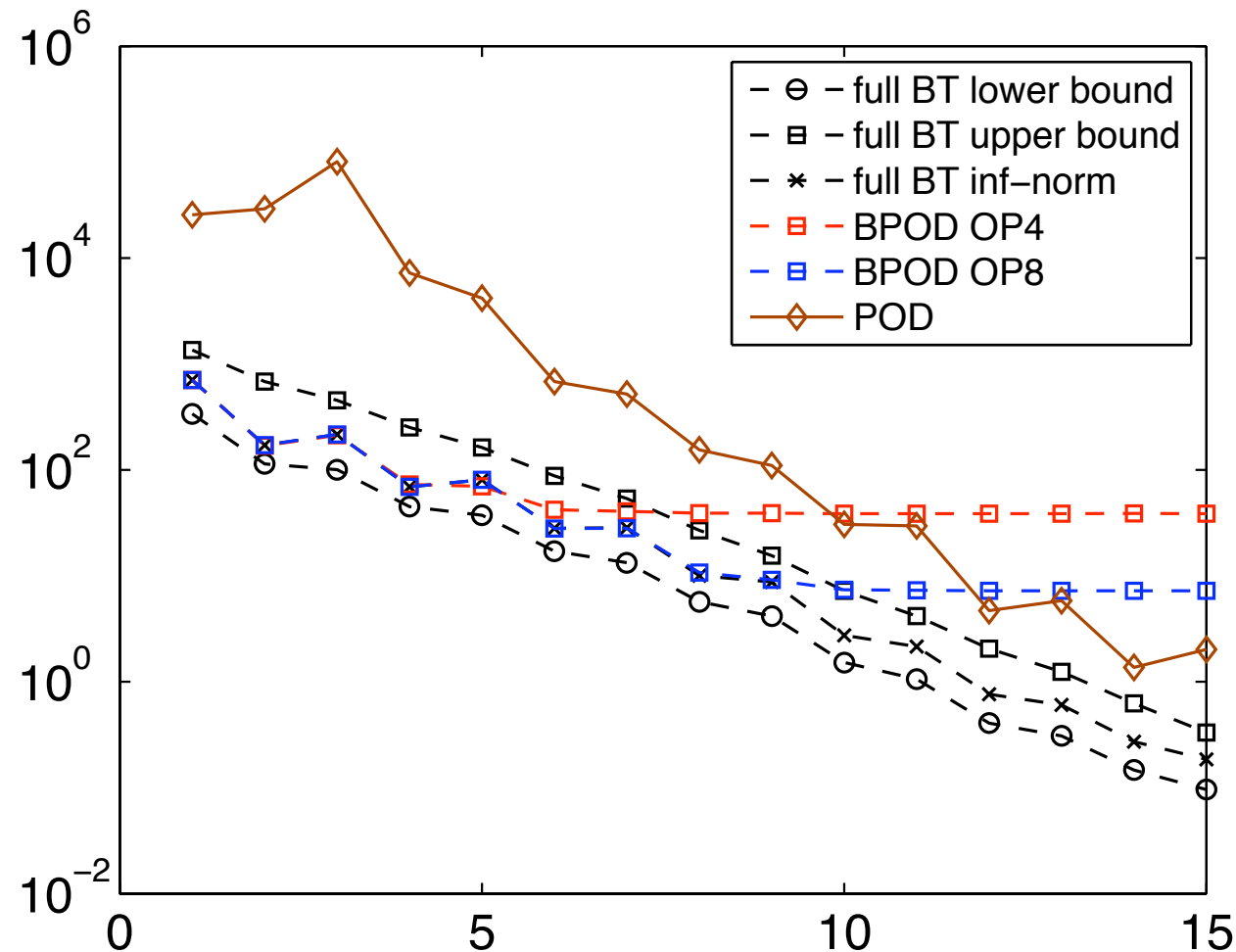
Single wavenumber - frequency response

- For a single wavenumber, frequency response can be computed exactly
- BPOD captures the resonant peak even at low order
- POD slowly improves with additional modes, but has **spurious peaks** due to eigenvalues near the imaginary axis



Single wavenumber - infinity norms

Infinity error norm bounds $\sigma_{r+1} \leq \|G - G_r\|_\infty \leq 2\sum_{j=r+1}^n \sigma_j$

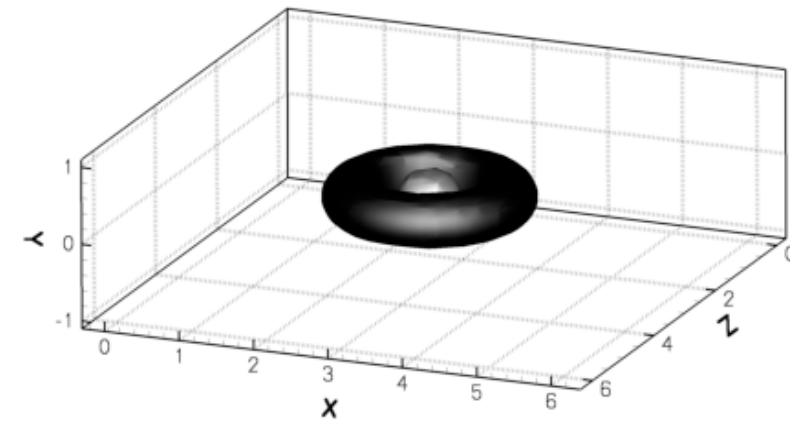


- Infinity norms of models also match those of exact BT up to approximately the rank of the output projection
- Again, POD ‘catches up’ only at a high rank

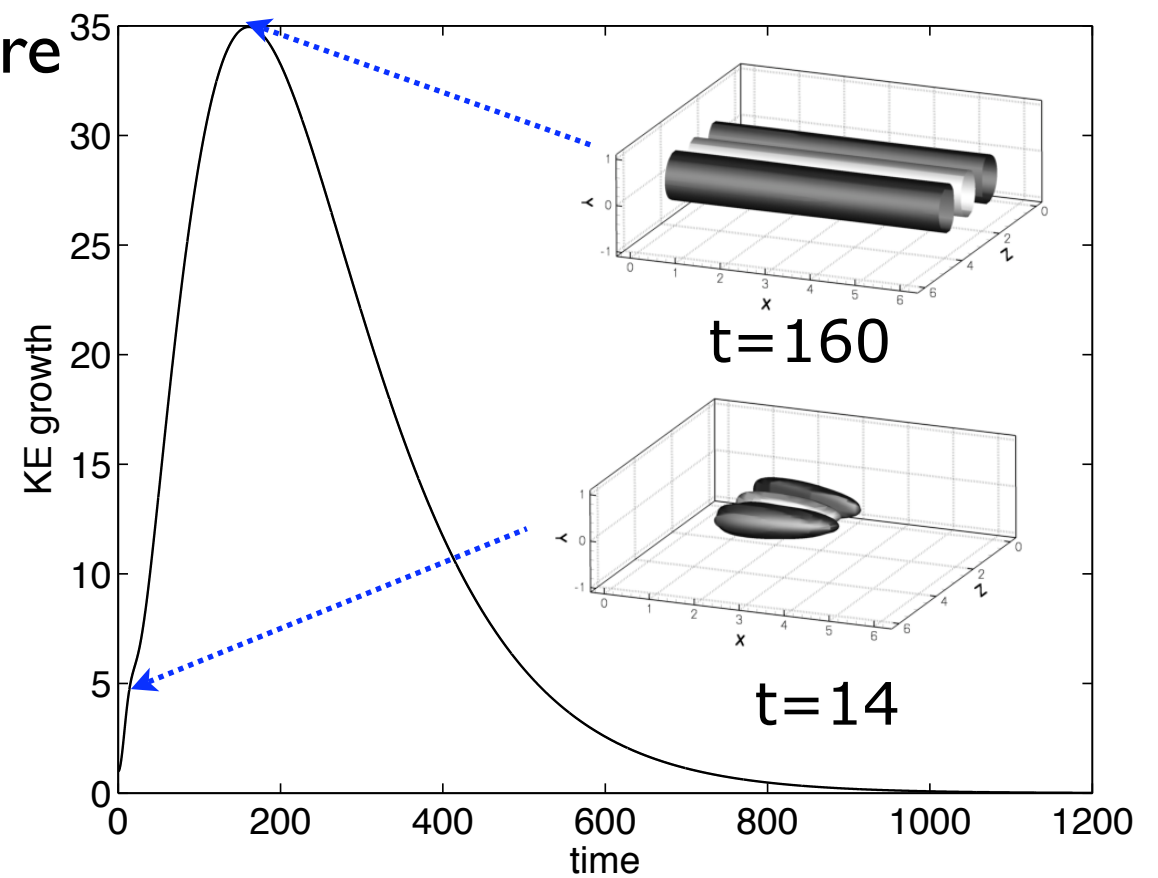
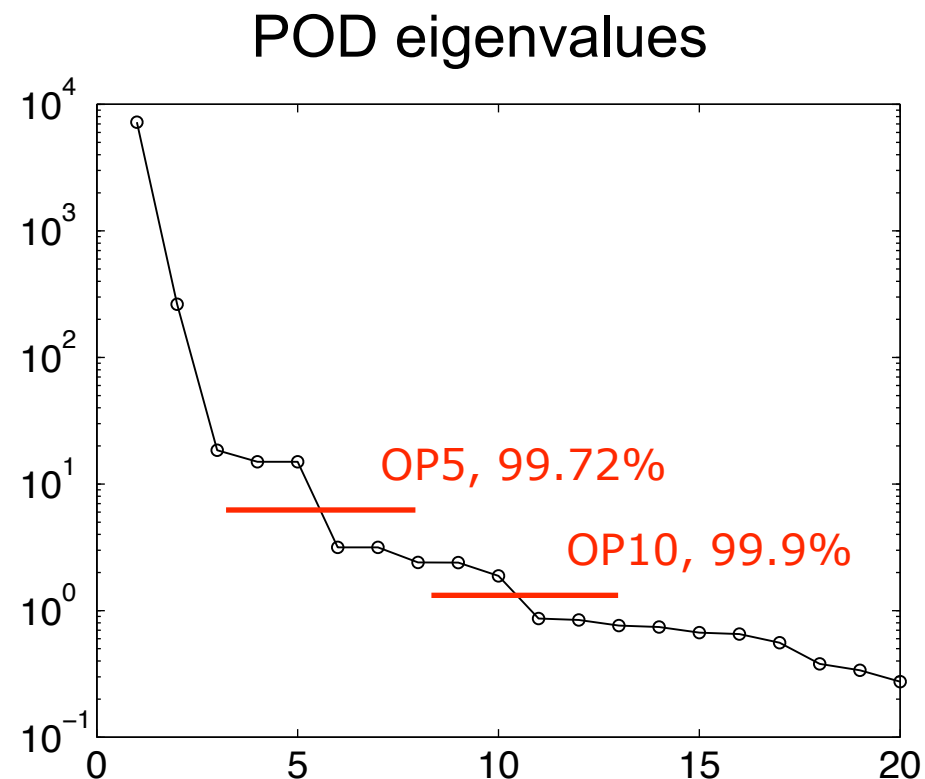


Localized actuator/disturbance

- Periodic array of localized disturbances in center of channel
- Large system (32x65x32), 133,120 states, exact BT intractable
- Impulse response snapshots obtained via linearized DNS, $Re=2000$
- Complex initial transient develops into a streamwise-constant structure

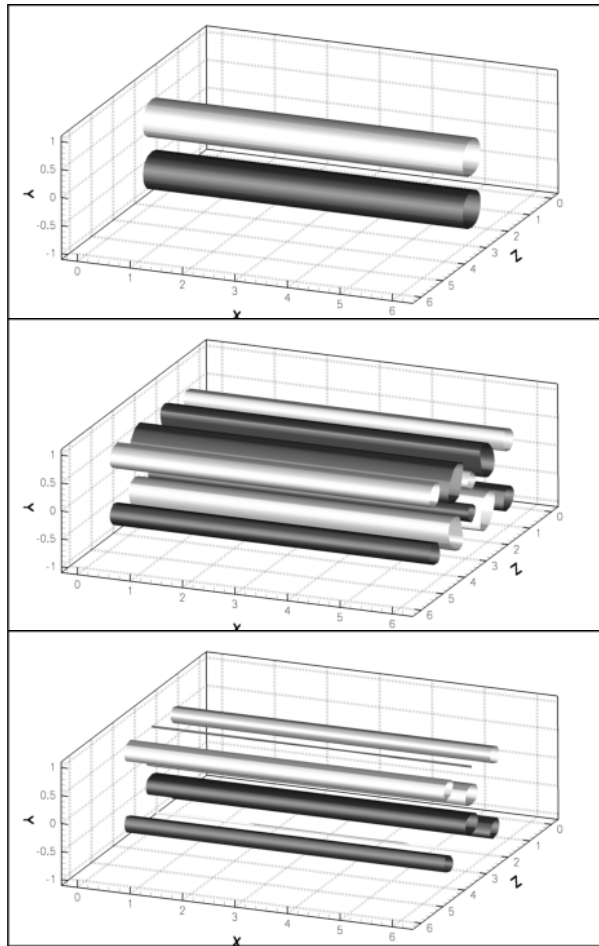


initial condition

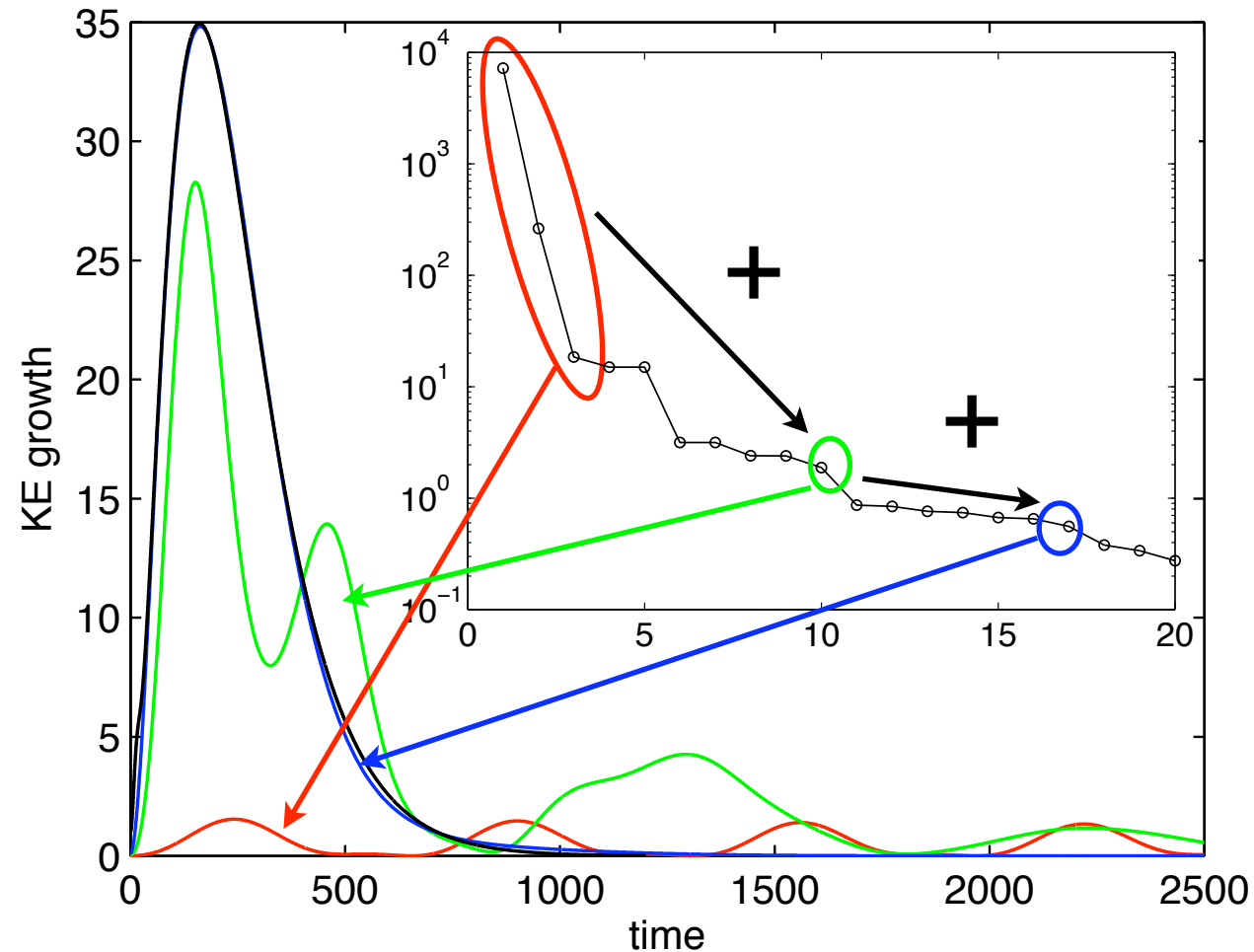


Localized actuator - POD model performance

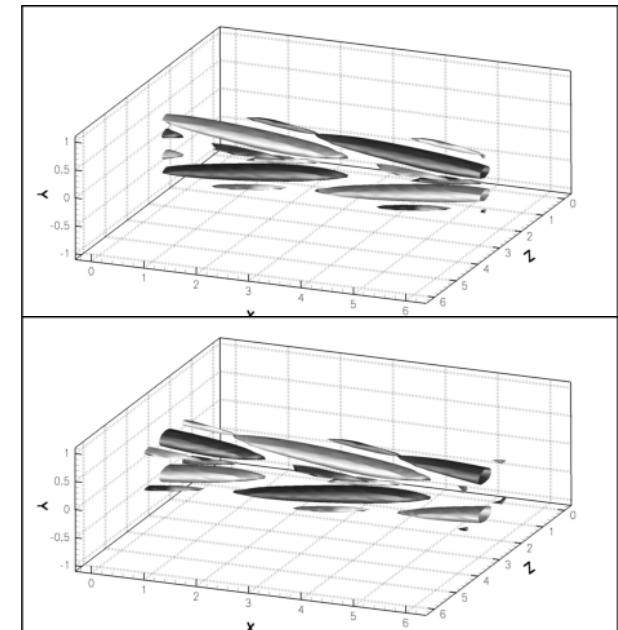
POD modes 1-3



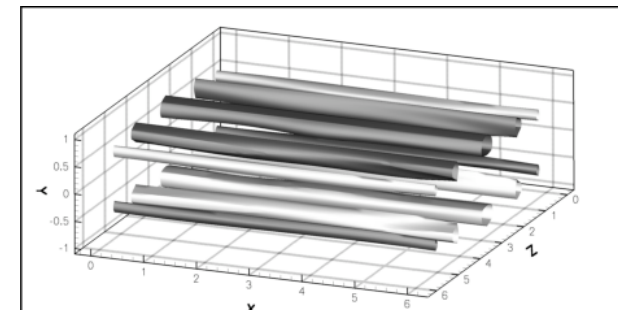
Standard POD



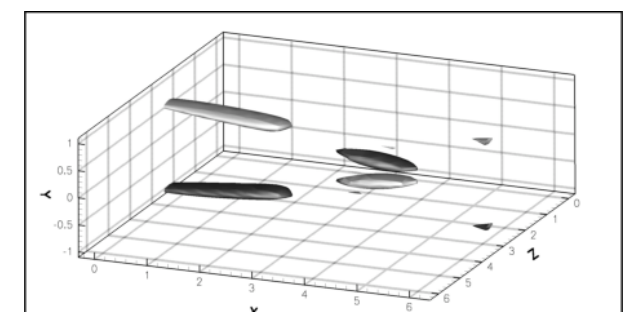
POD modes 4-5



POD mode 10



POD mode 17

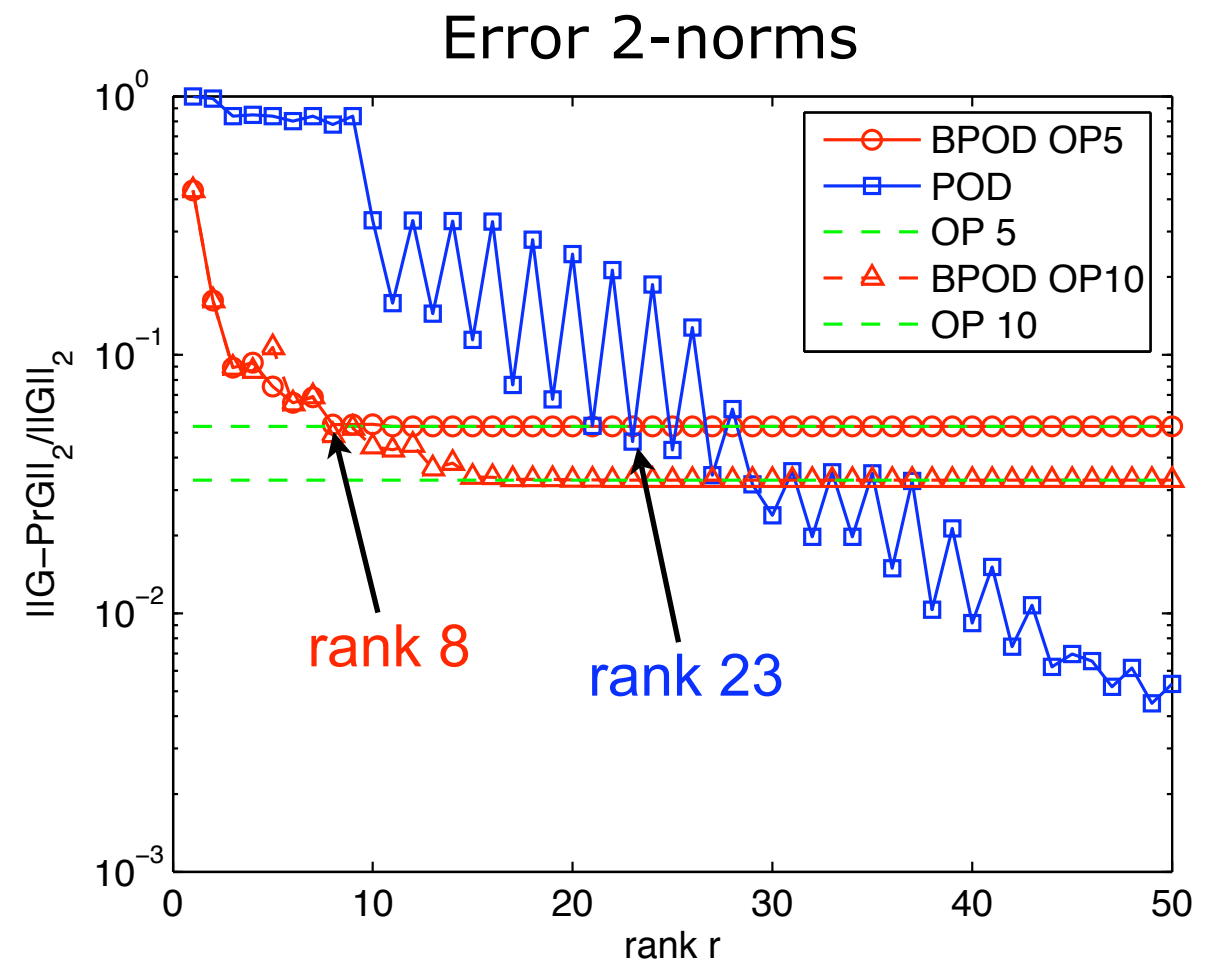
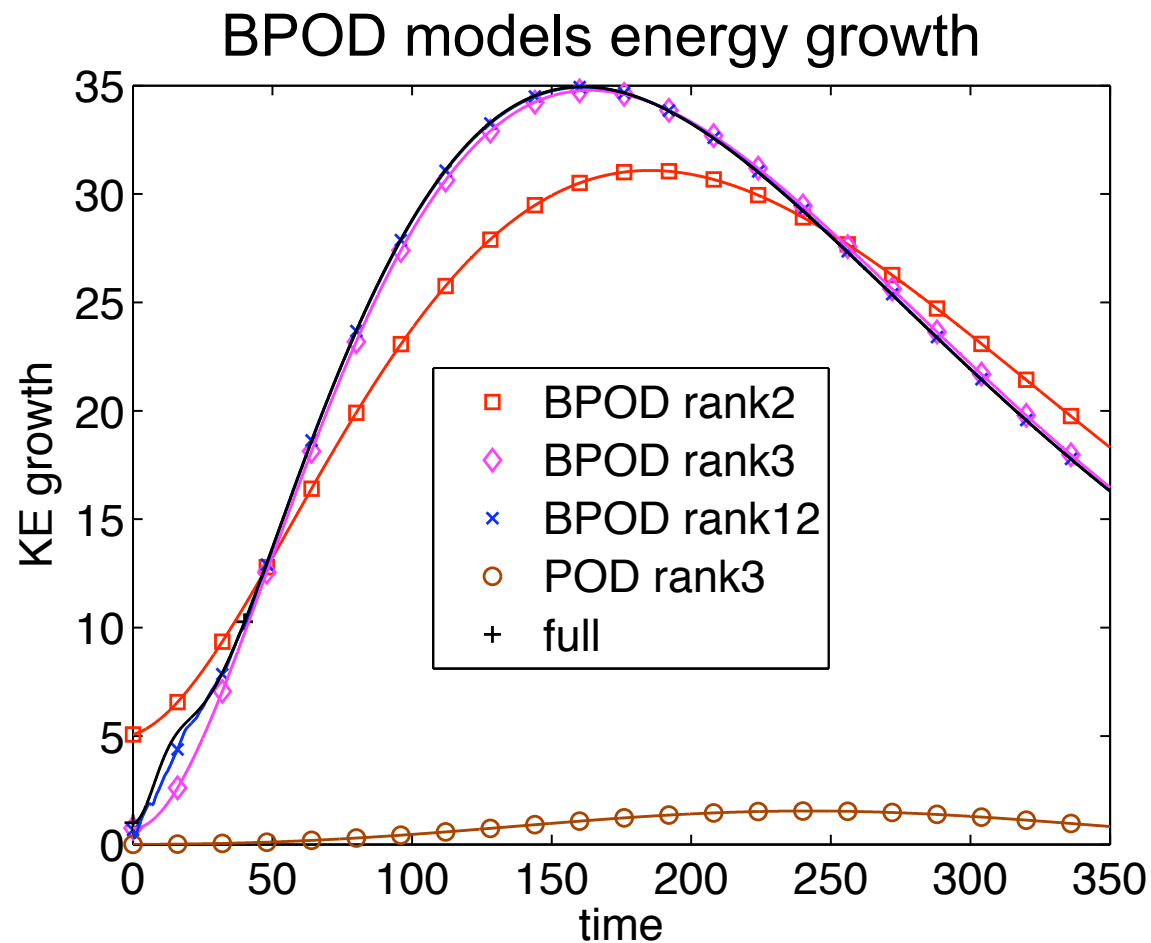


- 5-order model with modes 1,2,3,10,17 much better than 5-mode model with modes 1-5.

Conclusion: some low-energy POD modes are very important for the system dynamics. Can't naively use just the most energetic ones.



Localized actuator - BPOD impulse response

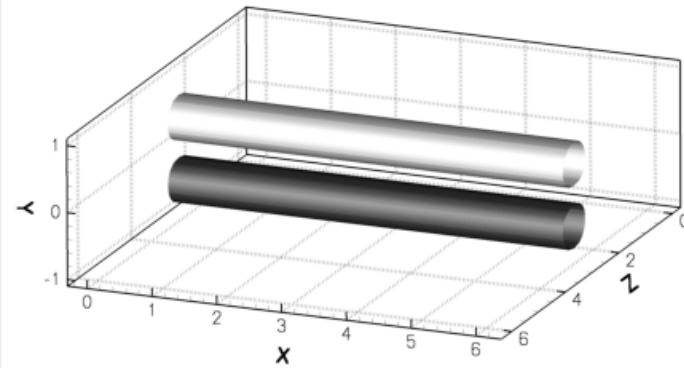


- Three-mode BPOD model excellent at capturing the energy growth
- Rank 8 BPOD model sufficient to correctly capture the dynamics of the first five POD modes, compared to at least 23 POD modes
- Inclusion of some POD modes significantly deteriorates performance (splitting of the pairs of oscillating modes)

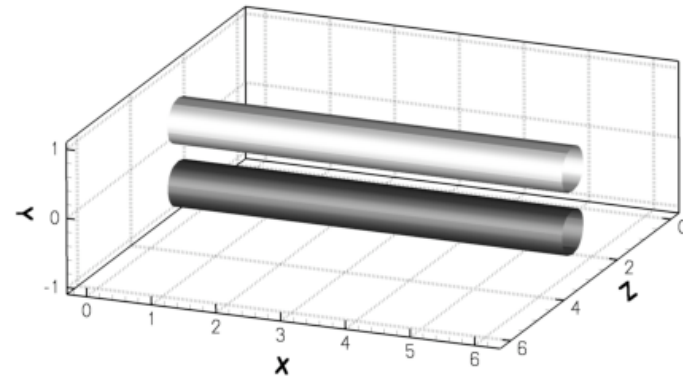


Localized actuator - modes

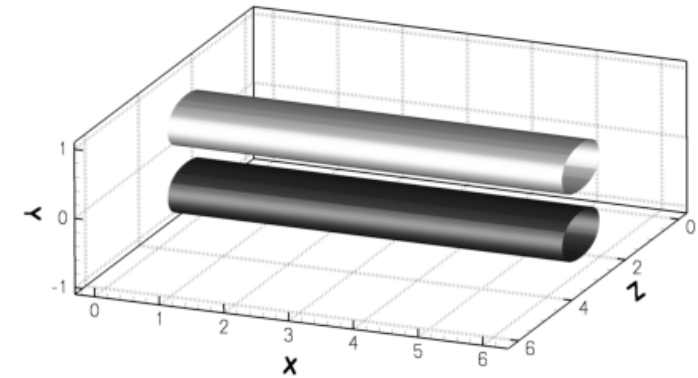
POD mode 1



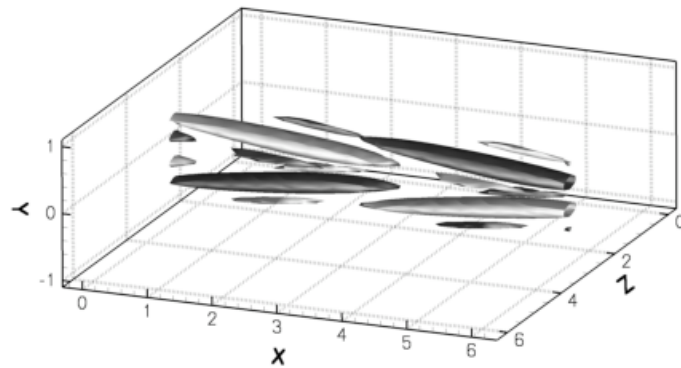
BPOD mode 1



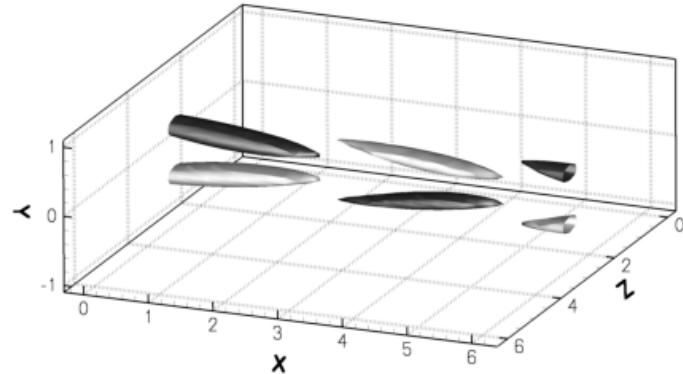
adjoint BPOD mode 1



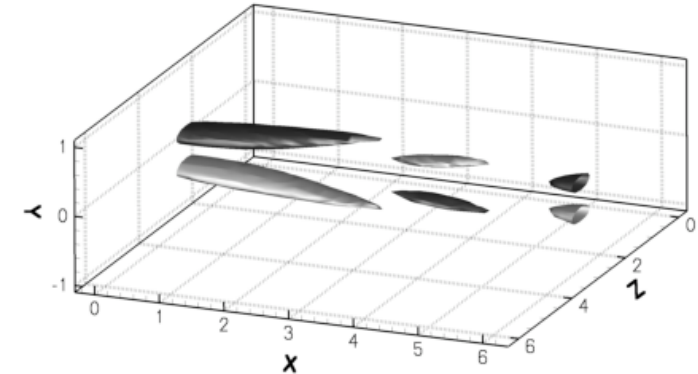
POD mode 4



BPOD mode 4



adjoint BPOD mode 4



BPOD and adjoint BPOD modes from OP5

Balancing modes and POD modes look similar but the adjoint modes are in general quite different => different dynamics of models

POD

$$\dot{a}_j(t) = \langle \underline{\phi}_j, f(x) \rangle$$

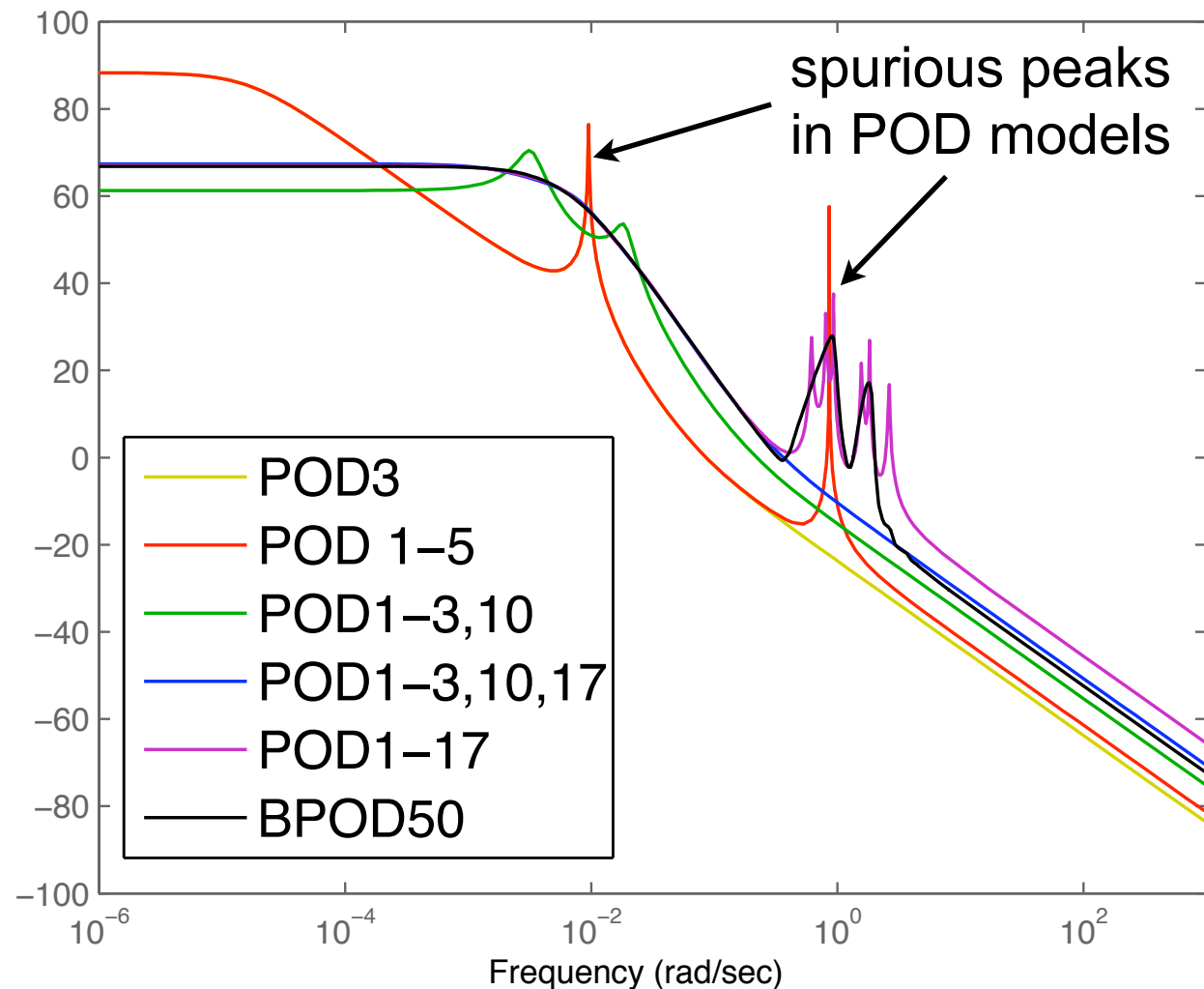
BPOD

$$\dot{a}_j(t) = \langle \underline{\psi}_j, f(x) \rangle$$

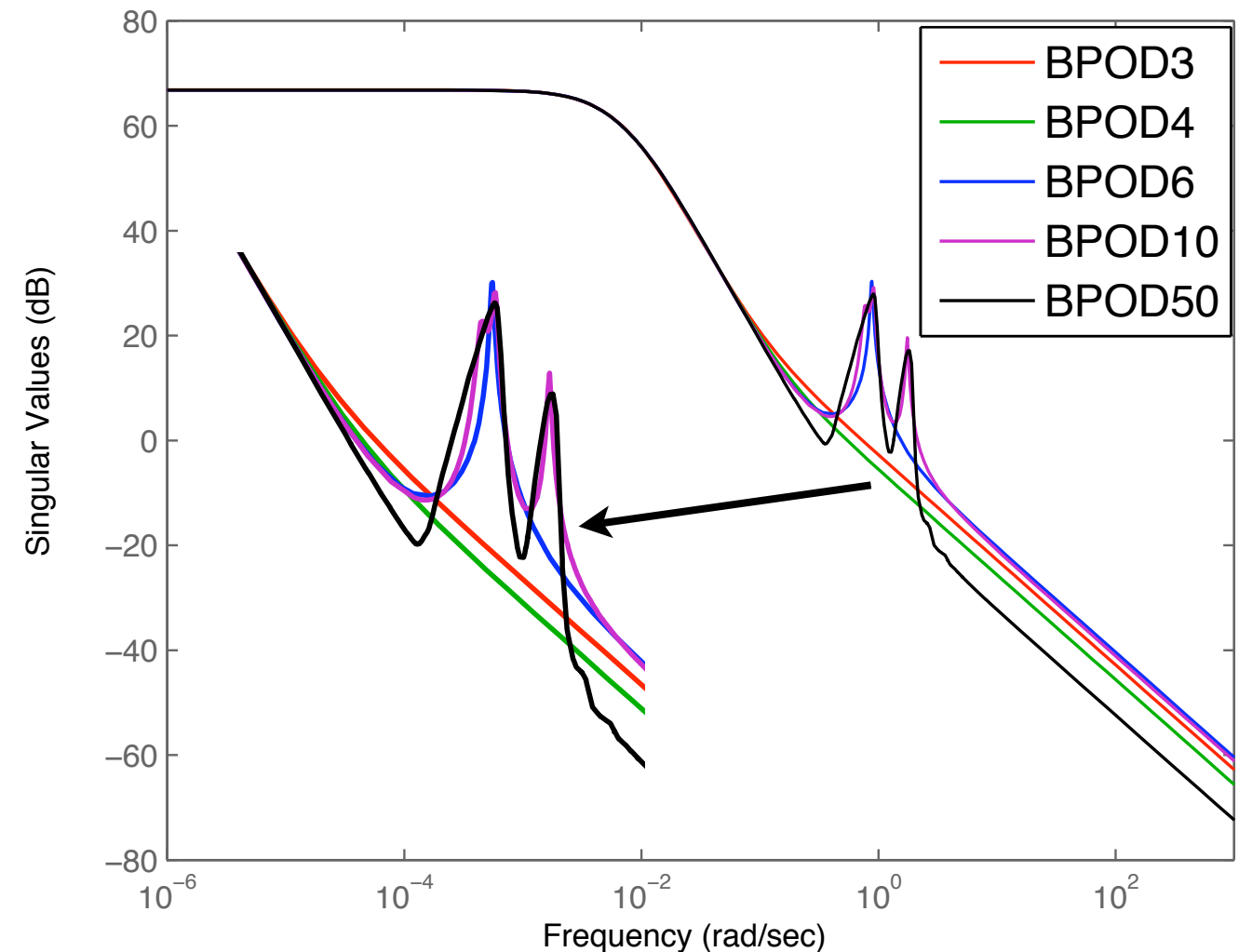


Localized actuator - frequency response

POD singular value Bode plot



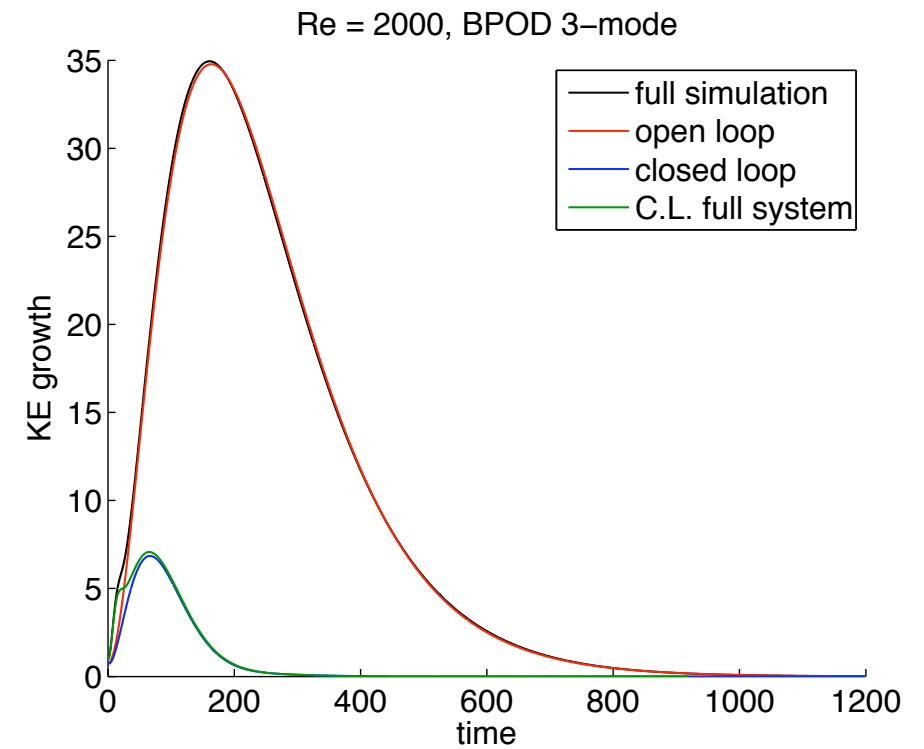
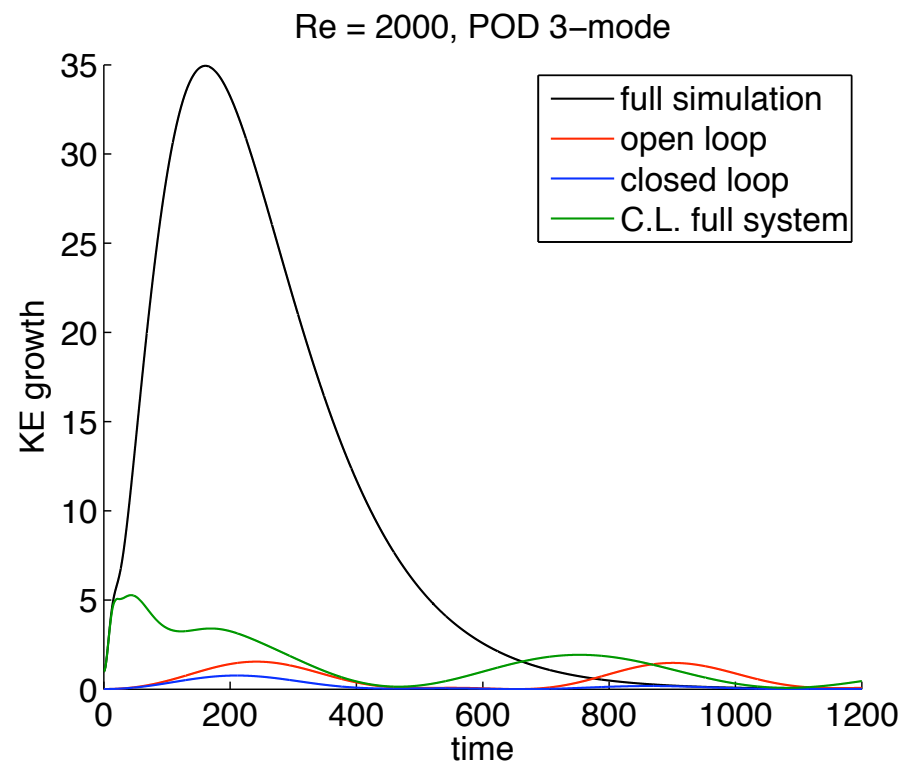
BPOD singular value Bode plot



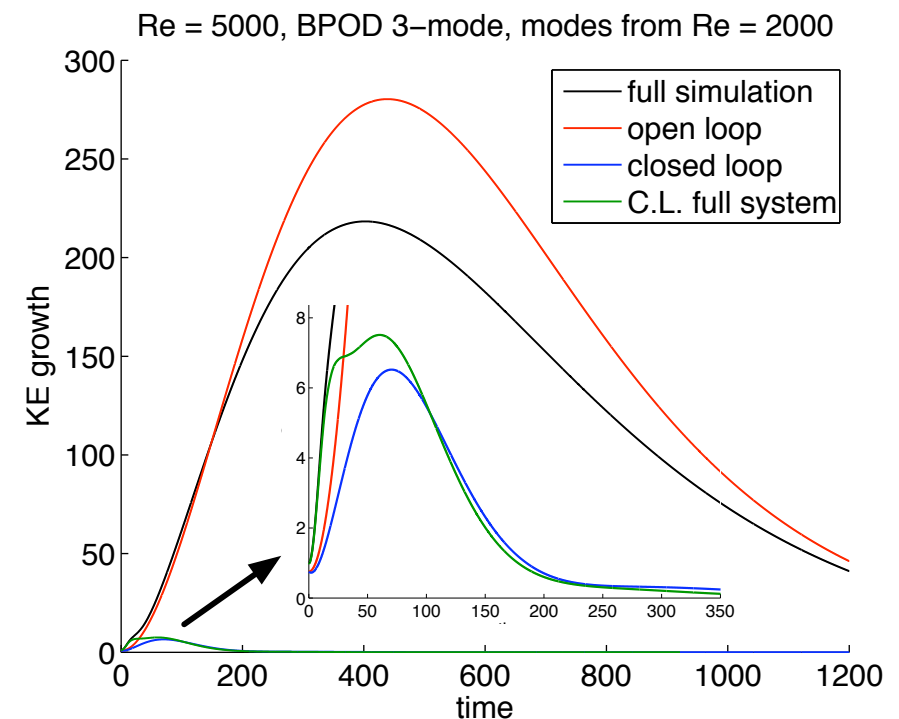
- BPOD 10-mode OP 50-mode model taken as 'full system'
- POD poorly captures low-pass behavior, spurious peaks
- Need pairs of BPOD modes to capture peaks



Closed-loop control - localized actuator

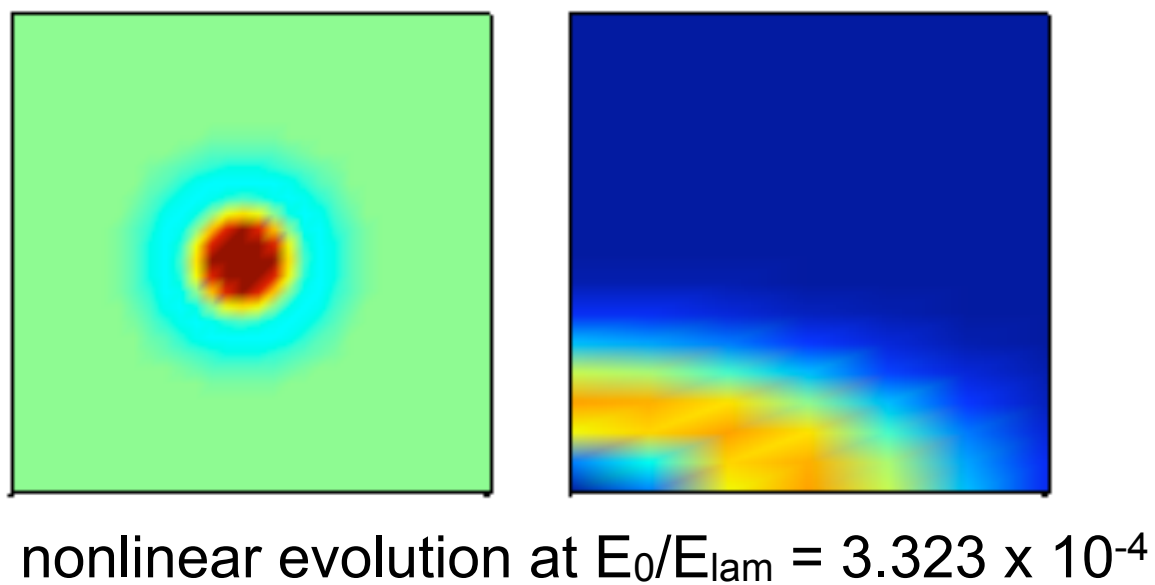
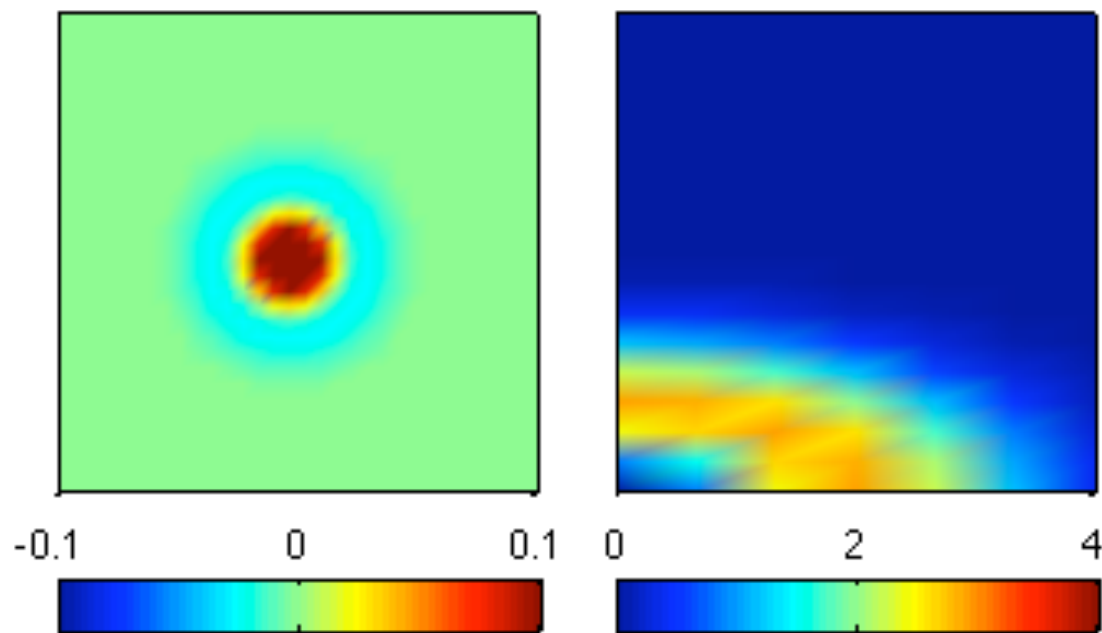


- Using the localized actuator to control a disturbance in channel center
- Standard LQR control design
- Using control gains from a 3-mode BPOD model reduces energy growth by a factor of 5



Nonlinear Evolution of the Localized Perturbation

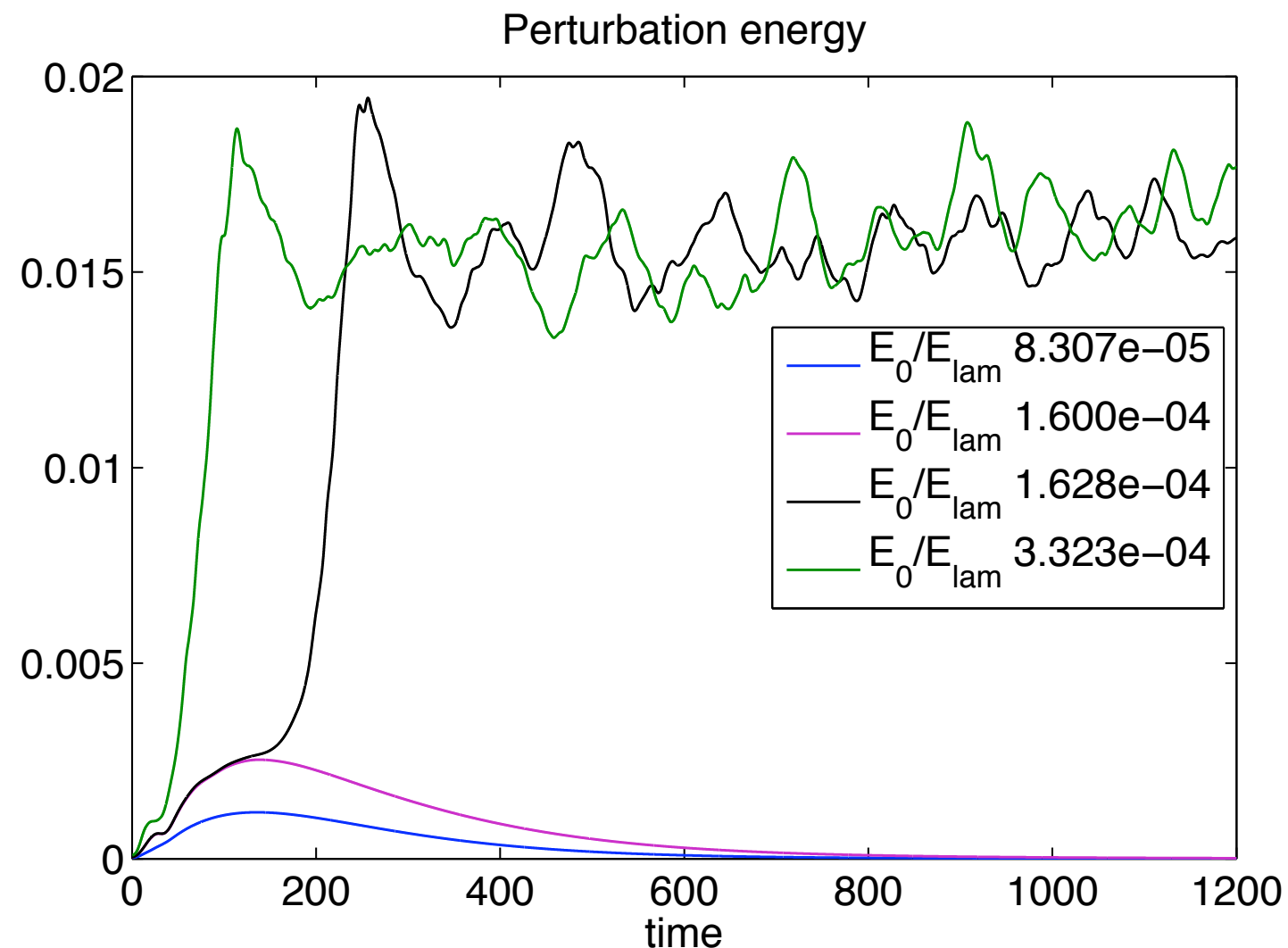
linear evolution of wall-normal velocity



- The spatial Fourier transform of the x,z plane at $y=0$ illustrates the perturbation evolution
- In the linear case the wavenumbers decay independently after the large transient growth
- $E_{\text{lam}} = 0.2667$ is the energy density of the mean laminar flow
- Transition for very small values of initial energy E_0
- The so-called β -cascade [Henningson et al, 1993] is observed in the nonlinear evolution - higher spanwise wavenumbers are introduced rapidly

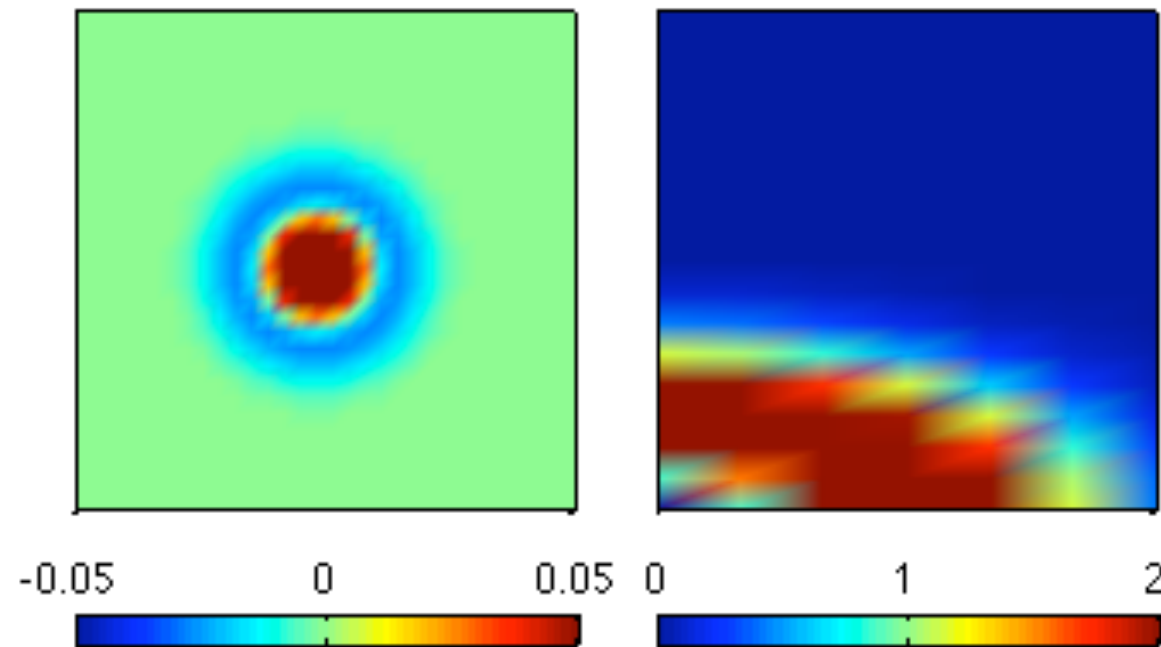
Delaying Transition Using Feedback Control

- Try to increase the transition threshold of a localized perturbation (after Reddy et al)
- The threshold is defined as the energy density of the initial perturbation above which the flow transitions to turbulence
- Threshold found to be at $E_0 = 1.614 \times 10^{-4}$ of the mean flow energy of the laminar profile, $E_{\text{lam}} = 0.2667$



Closed-Loop Control

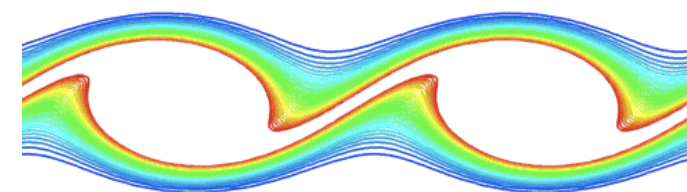
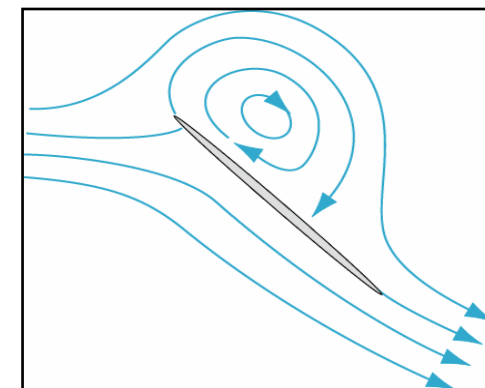
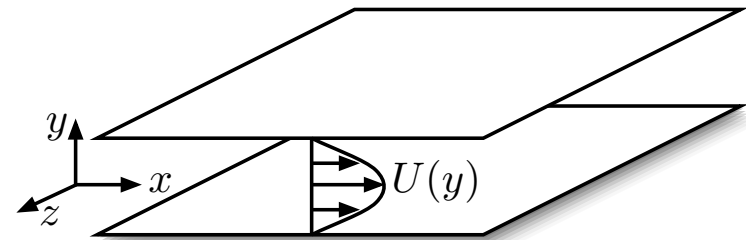
- The feedback gains computed using LQR for the linear system are used in a full nonlinear simulation with $E_0/E_{lam} = 3.323 \times 10^{-4}$
- An ‘aggressive’ controller ($R=0.1$ in LQR) manages to suppress the disturbance



- Explanation: the BPOD modes do not have components at high β , and are not able to suppress high betas once they arise, but the ‘aggressive’ controller suppresses low β wavenumbers so that the higher β ’s emerge at very low amplitudes and decay linearly
- Transition threshold increased by a factor of 17 for $R=0.01$
- Work in progress: see how projection of full N-S equations onto linear BPOD modes will model the perturbation evolution, and possibly design a nonlinear controller

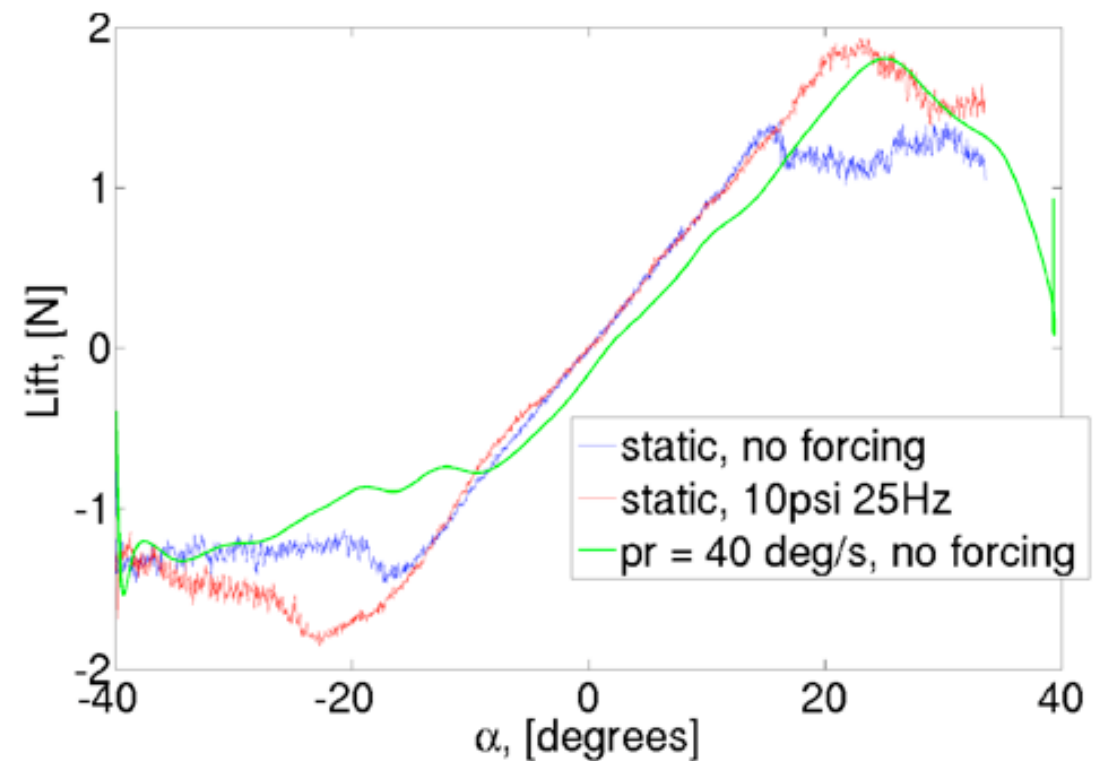
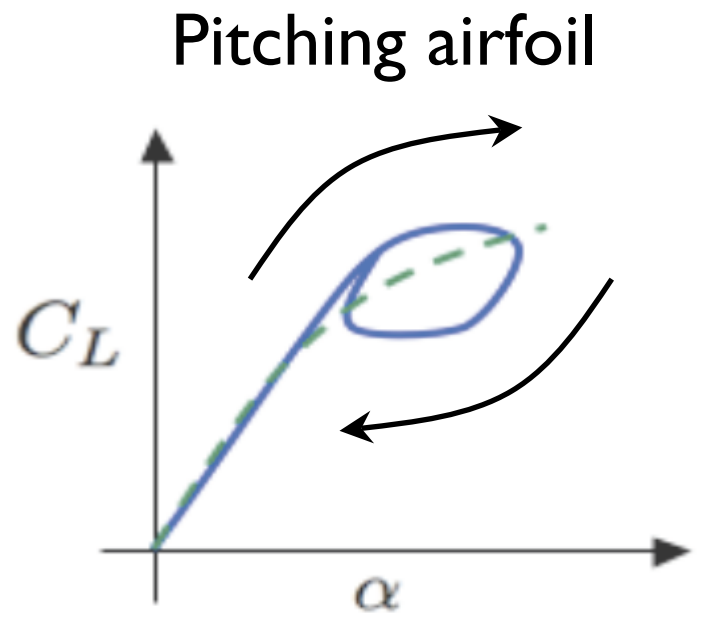
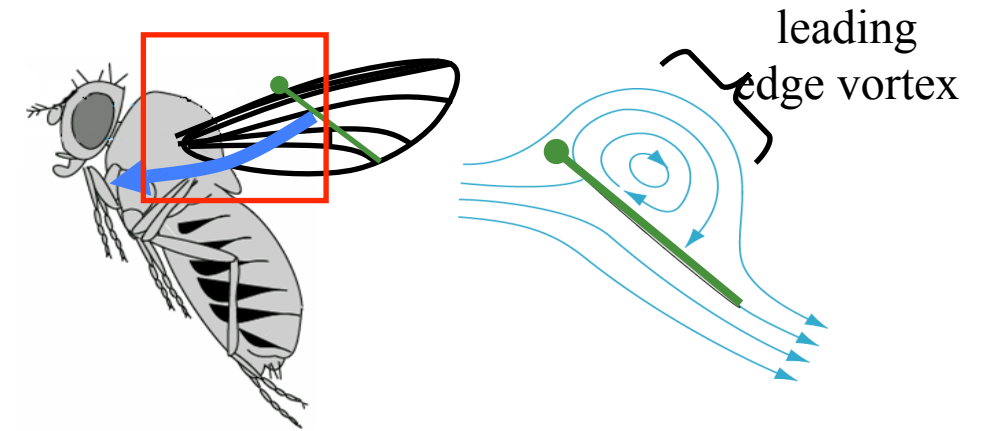
Outline

- Reduced-order models: POD and balanced truncation
 - Importance of inner product for Galerkin projection
 - Balanced truncation
 - Method of snapshots
- Applications
 - Linearized channel flow
 - Separating flow past an airfoil
- Dynamically scaling POD modes
 - Free shear layer
 - Scaled basis functions
 - Template fitting
 - Equations for the shear layer thickness



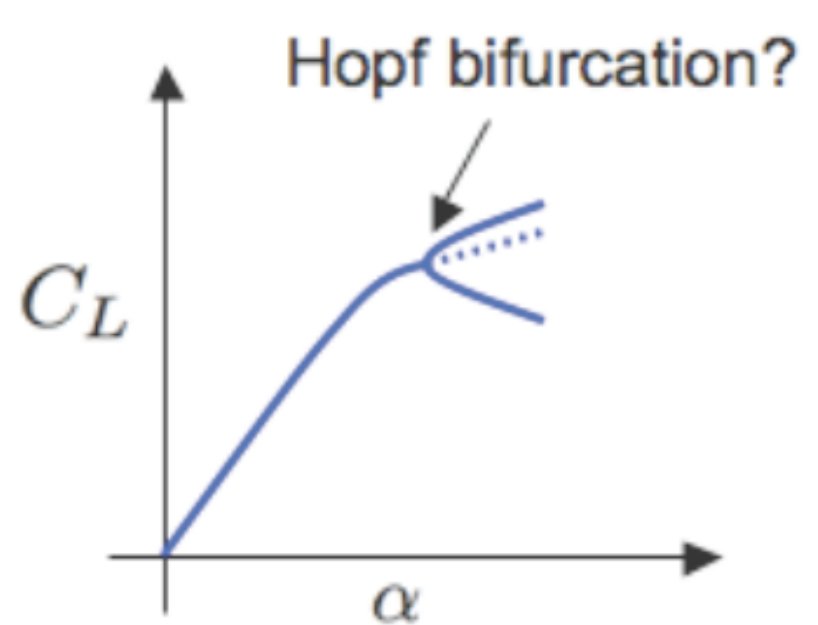
Motivation

- Leading edge vortices can provide high lift
- MURI with Caltech (Colonius), IIT (Williams), and Northeastern (Tadmor)
- Goal: Stabilize these LEVs using feedback control
- High transient lift in pitching airfoils due to dynamic stall vortex

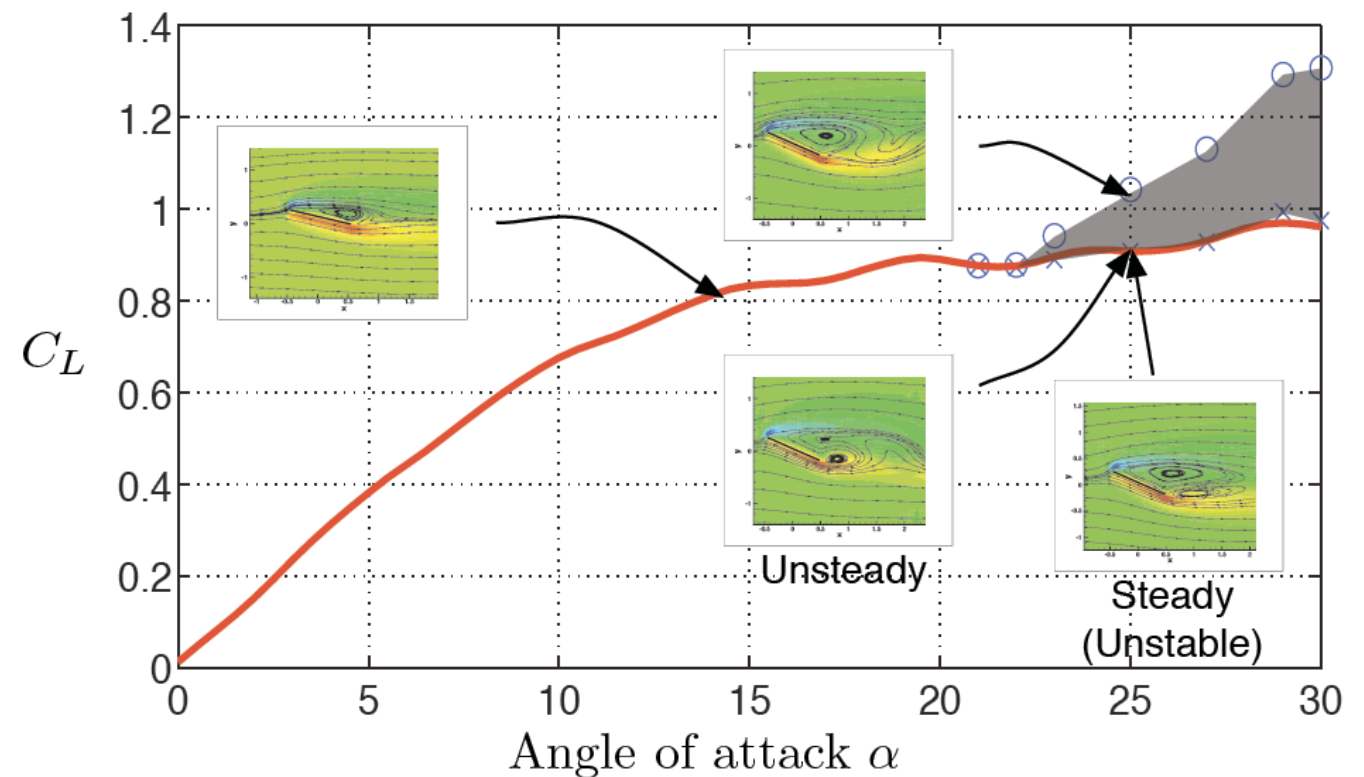


Dynamical behavior

- With increasing AoA, flow undergoes a Hopf bifurcation
- Reduced order models to stabilize unstable steady states at high AoAs



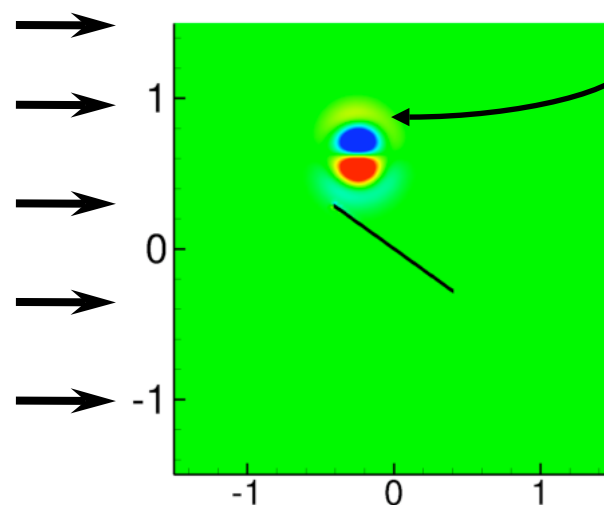
C_L at steady state



Are there high-lift unstable steady states in low aspect ratio airfoils?

Model problem

$Re = 100$
 $AoA = 25$ or 35



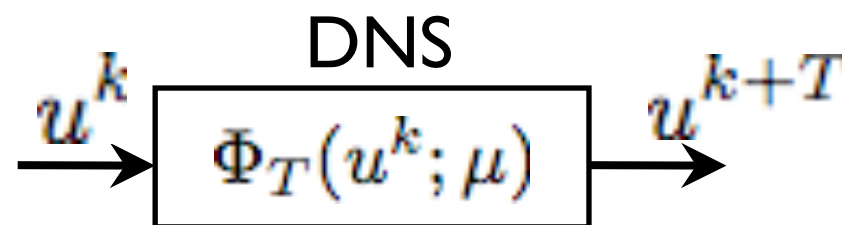
Actuator: localized
body force

- A fast null-space based immersed boundary scheme for numerical simulations

(T. Colonius and K. Taira, CMAME, 2007)

Steady state analysis

- Compute steady states using a wrapper around the DNS



Define: $g(u) = u^T - u$

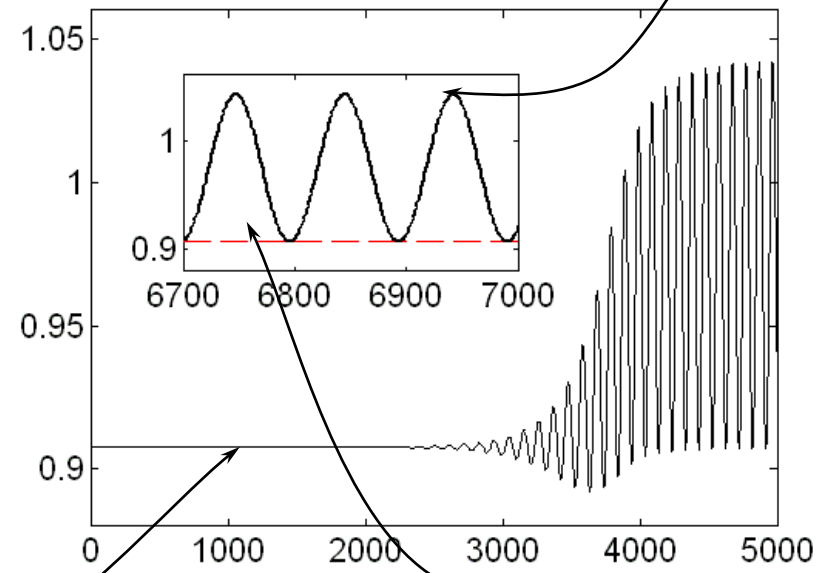
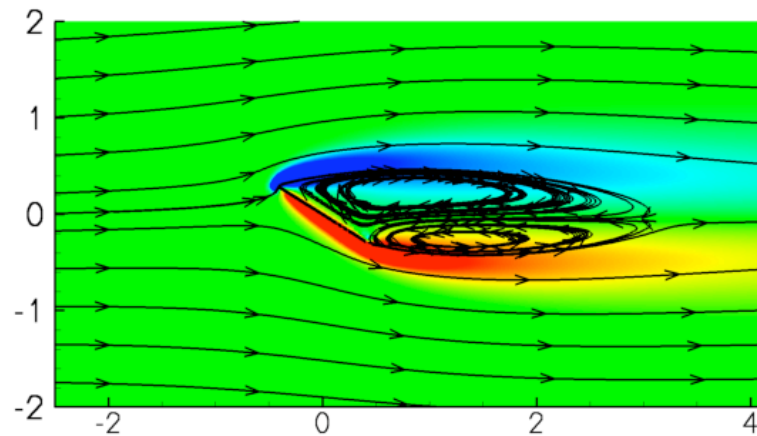
- Solve for zeroes of $g(u)$ using Newton-GMRES



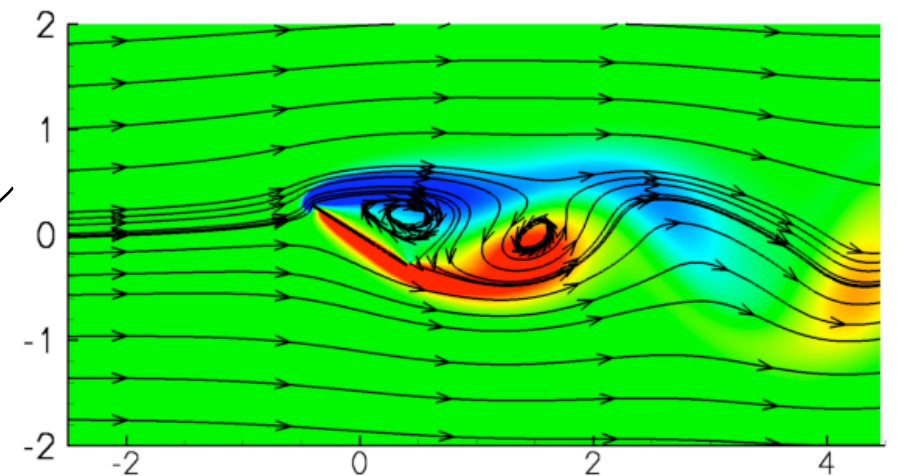
Unstable steady state, $AoA = 35$

- Steady state lift close to the min. lift of the unsteady case
- No leading edge vortex
- Trailing edge vortex causes reduced lift

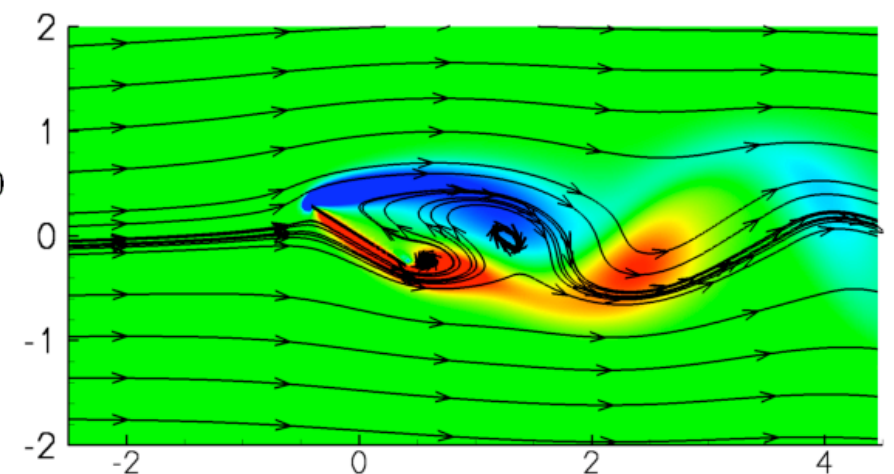
Steady, unstable



Unsteady, max lift

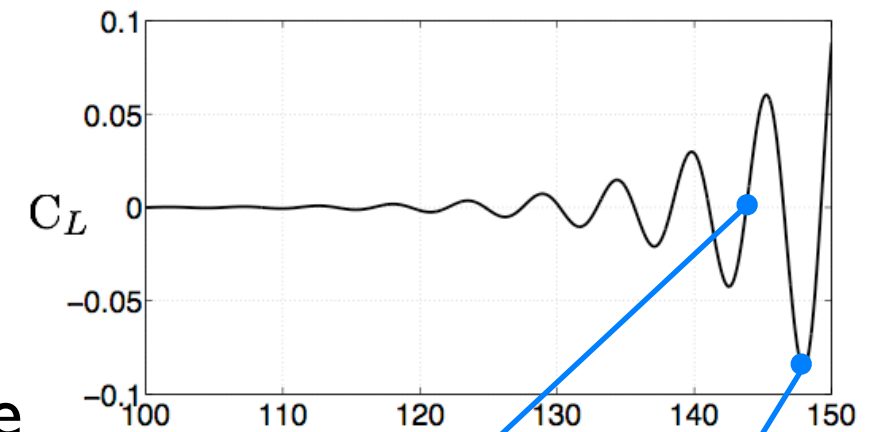


Unsteady, min lift

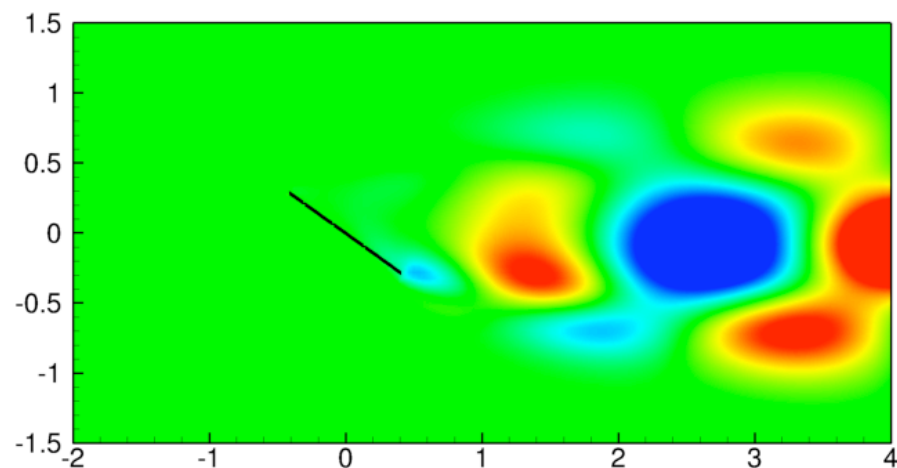
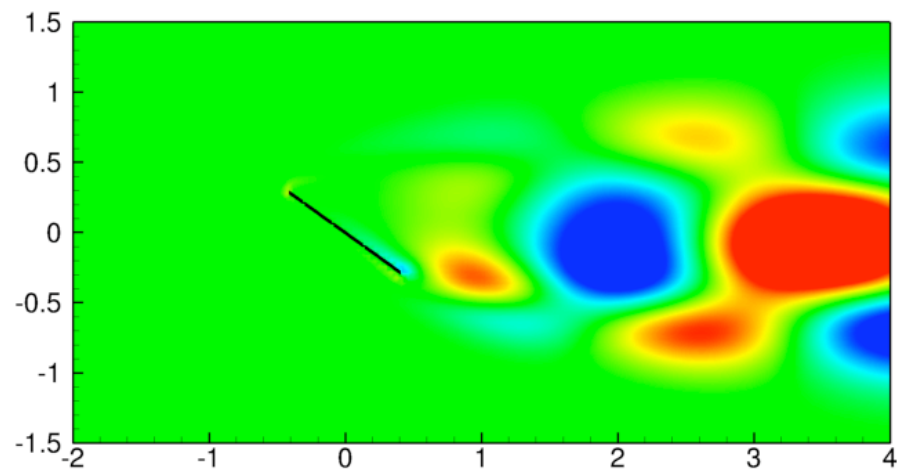


Linear stability analysis

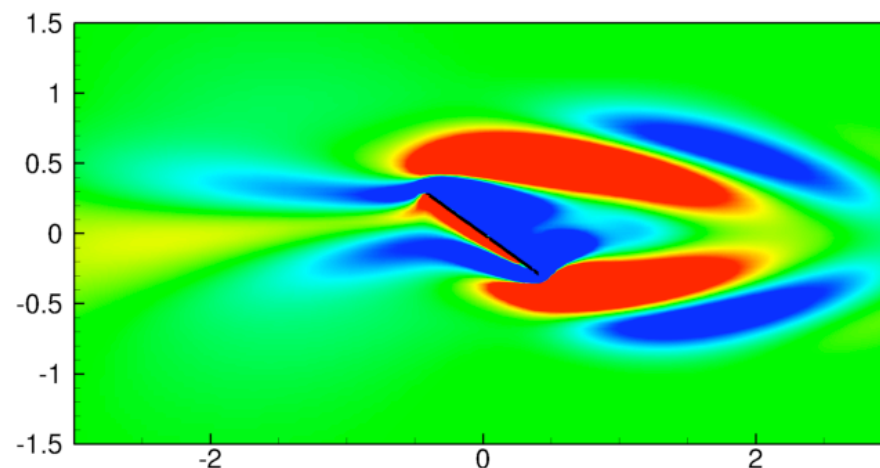
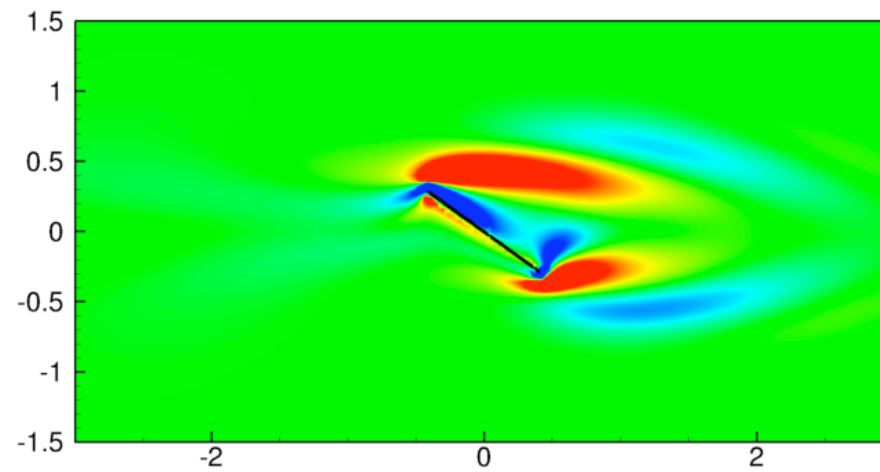
- Find the basis spanning the unstable eigenspace of the linearized and adjoint flows
- Run the linear simulations with a zero initial condition + 10^{-8} random noise



Right eigen-space



Left eigen-space

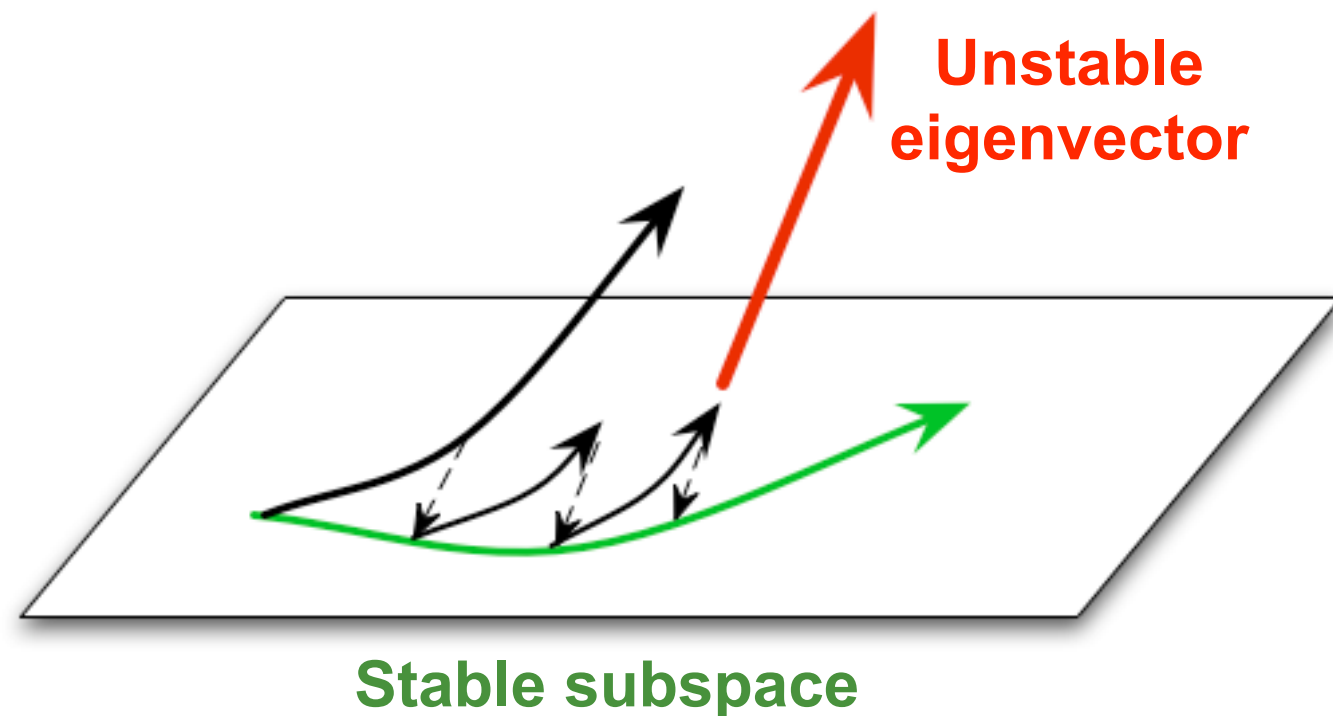


Reduced-order models for unstable systems

- Decouple stable and unstable subspaces
- Obtain balancing transformation for the stable subspace

$$\frac{d}{dt} \begin{pmatrix} x_s \\ x_u \end{pmatrix} = \begin{pmatrix} A_s & 0 \\ 0 & A_u \end{pmatrix} \begin{pmatrix} x_s \\ x_u \end{pmatrix} + \begin{pmatrix} B_s \\ B_u \end{pmatrix} u$$

- Snapshot based procedure: project out the unstable component at each time step

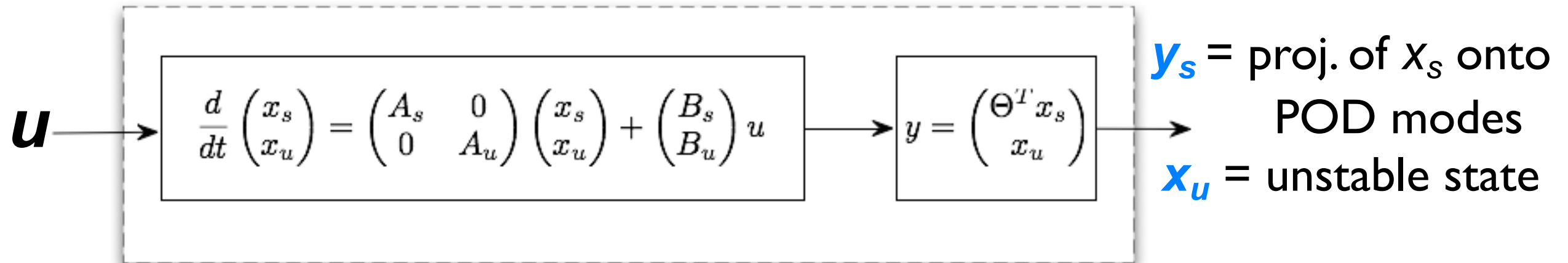


Balanced truncation for unstable systems, Zhou et al., '99



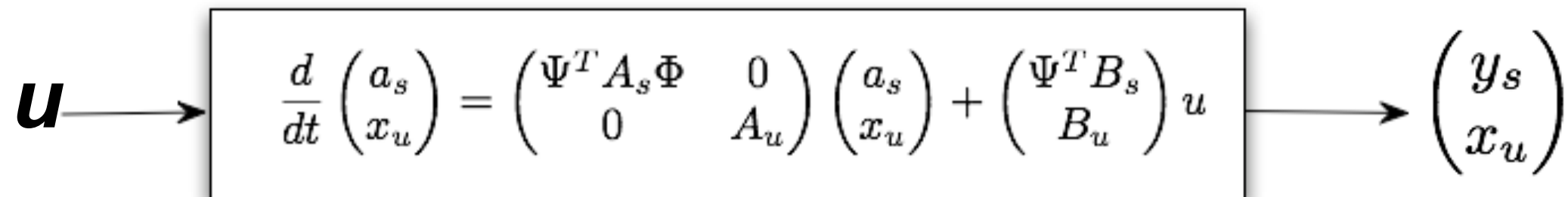
Model reduction: unstable system

Linearized NS eqns, 10^5



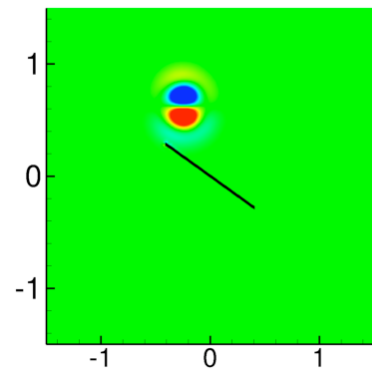
$$\begin{aligned} x_s &= \Phi a_s \\ \Psi^T \Phi &= I \end{aligned}$$

Reduced order model, 10-50 eqns.

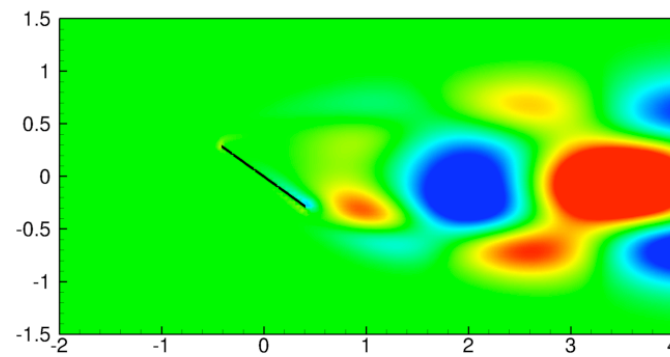


Impulse response: stable subspace

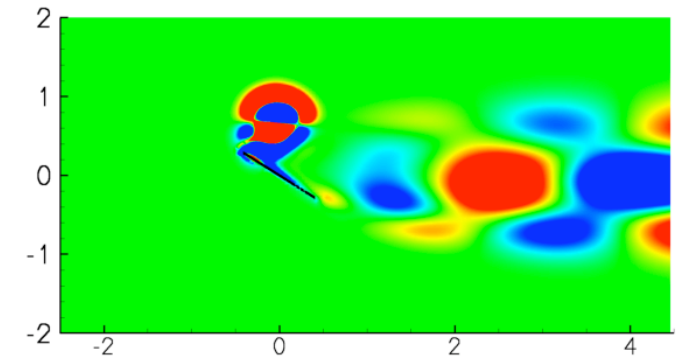
- Project out the unstable component from the initial condition



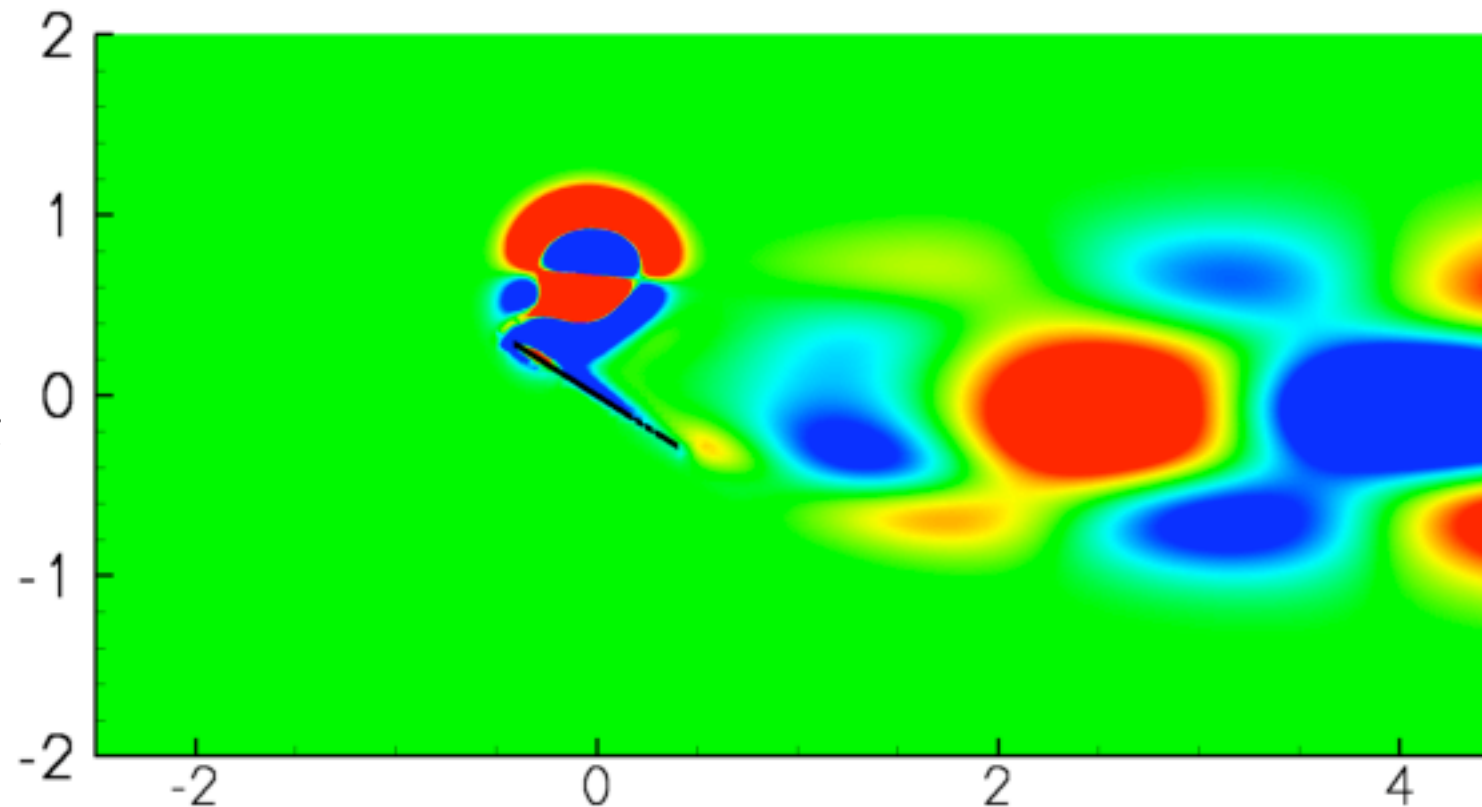
−



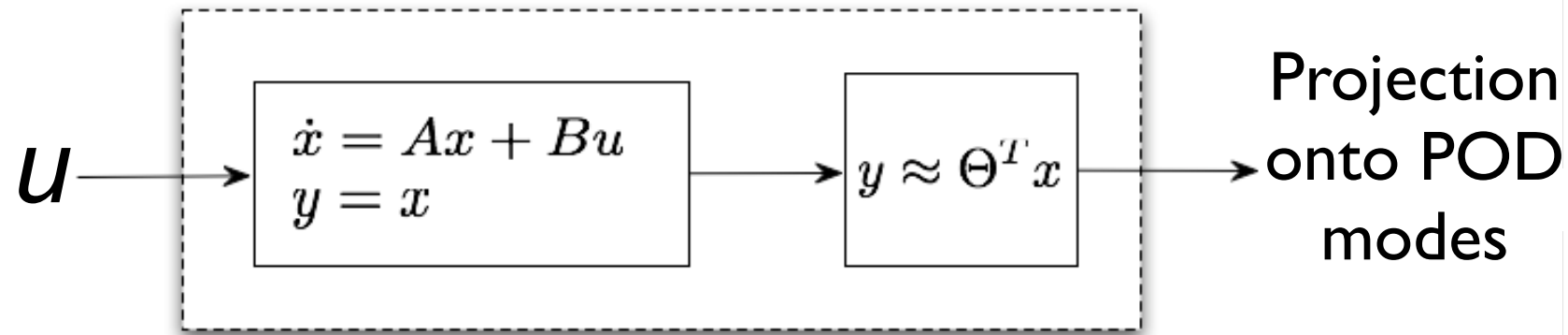
=



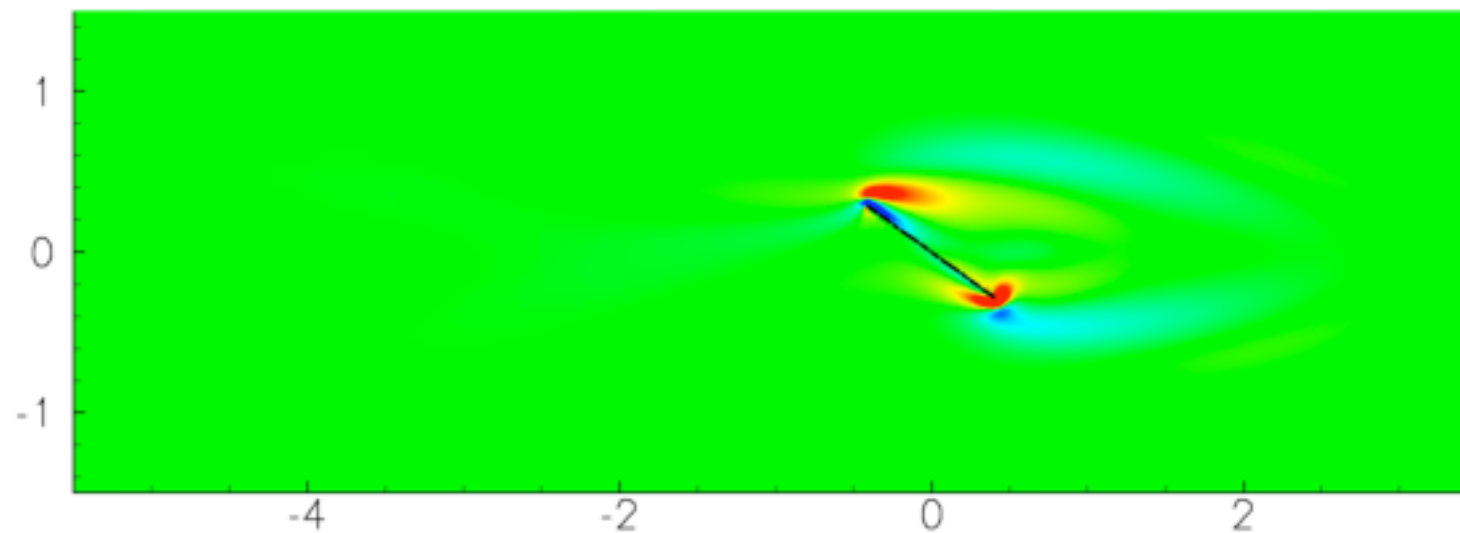
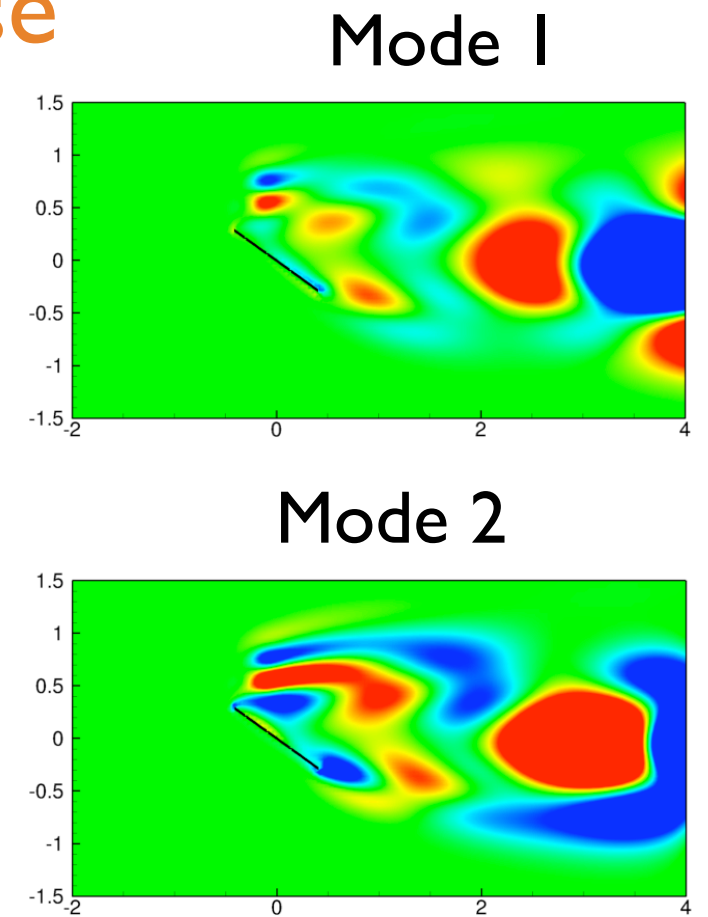
Vorticity contours:
Positive in red and
negative in blue



Adjoint impulse response



- Four POD modes capture 95% energy
- Adjoint solves with these POD modes as initial conditions

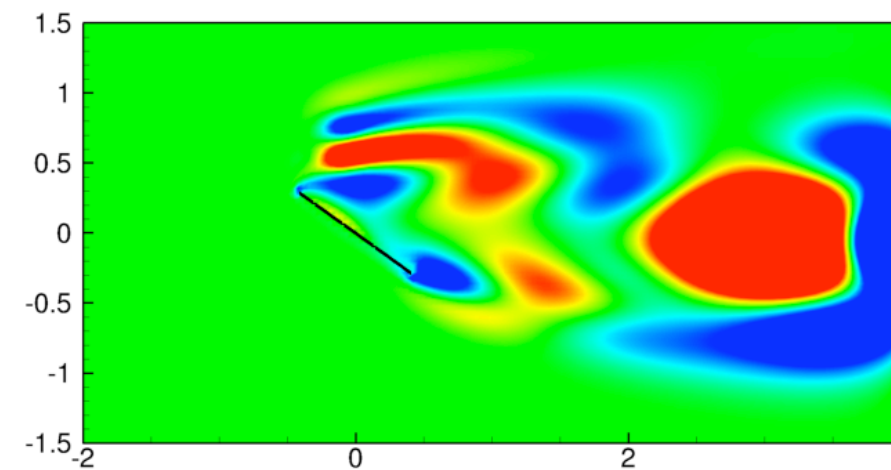
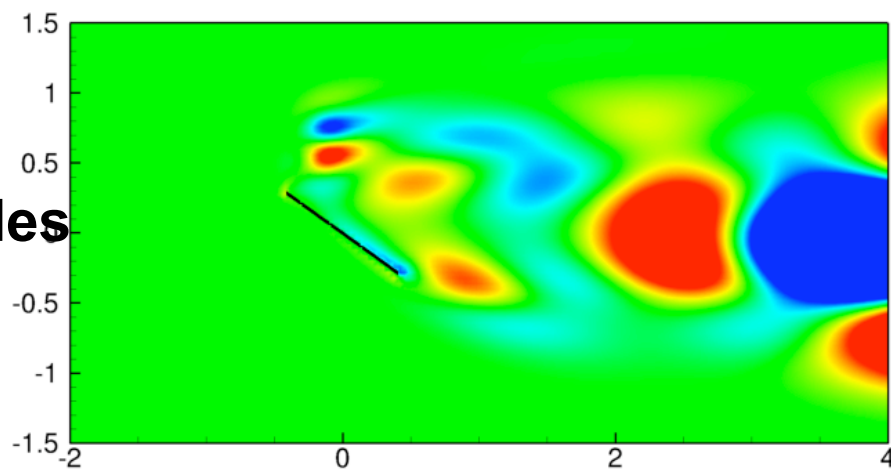


Balancing modes: stable subspace

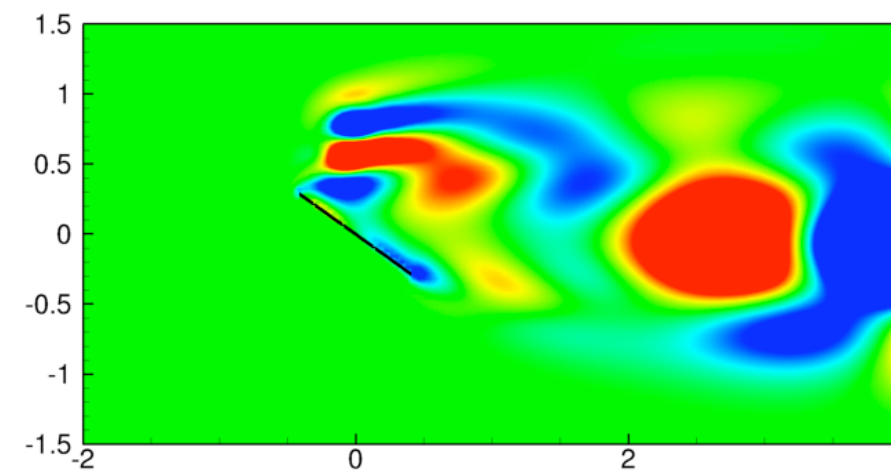
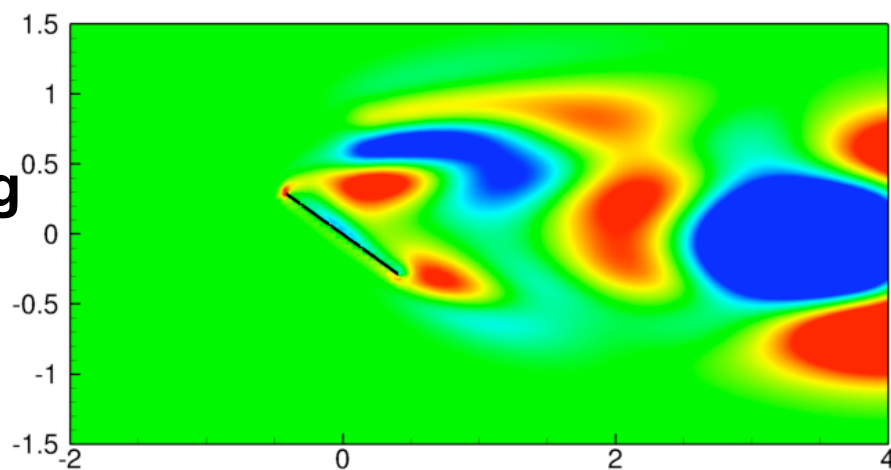
Mode 1

Mode 2

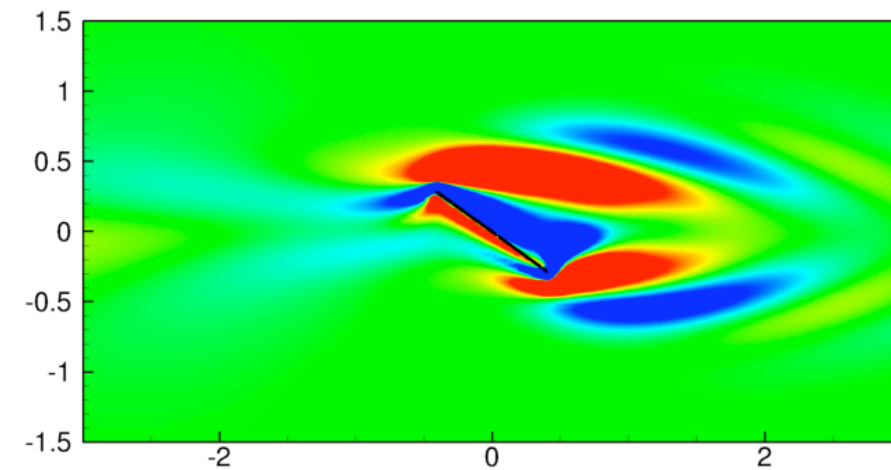
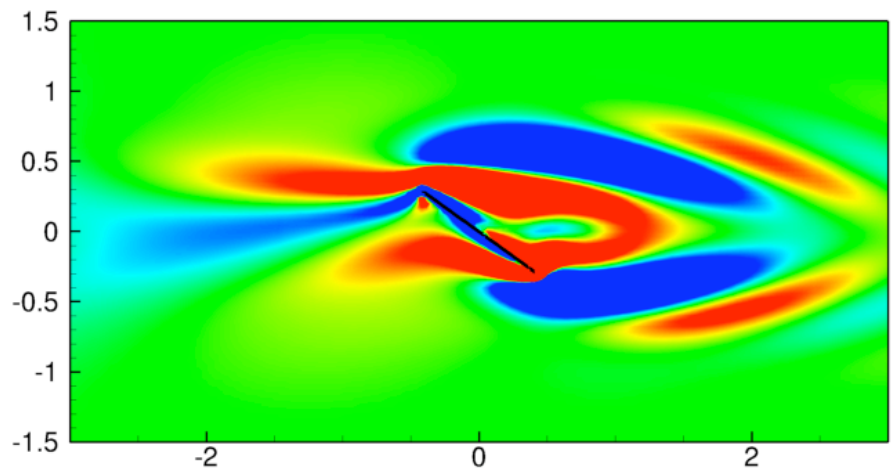
POD modes



Balancing modes



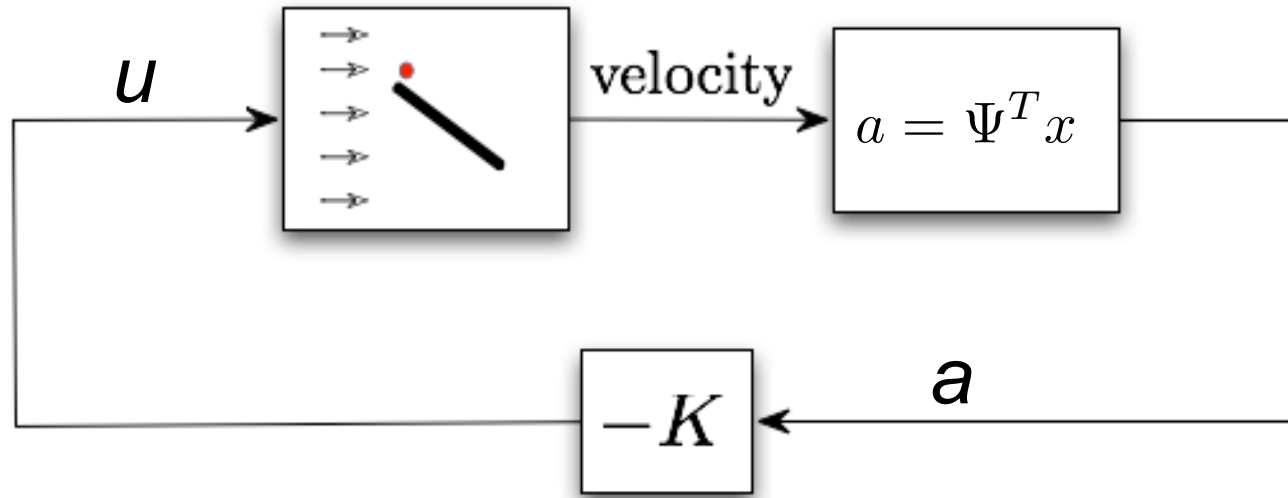
Adjoint modes



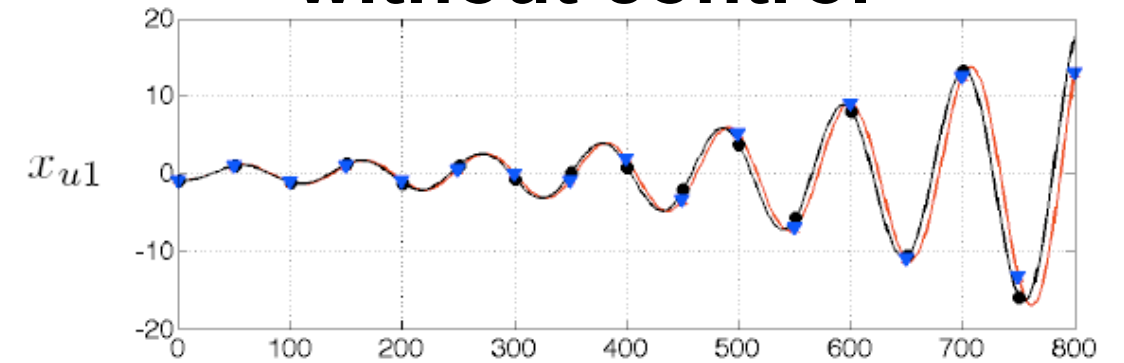
Bi-orthogonal



Model results: controlled case

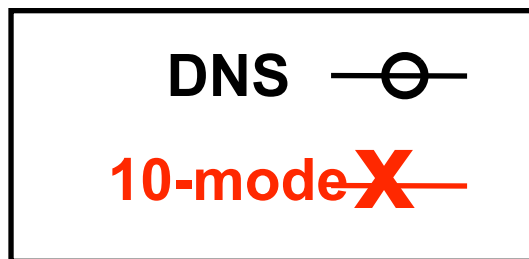
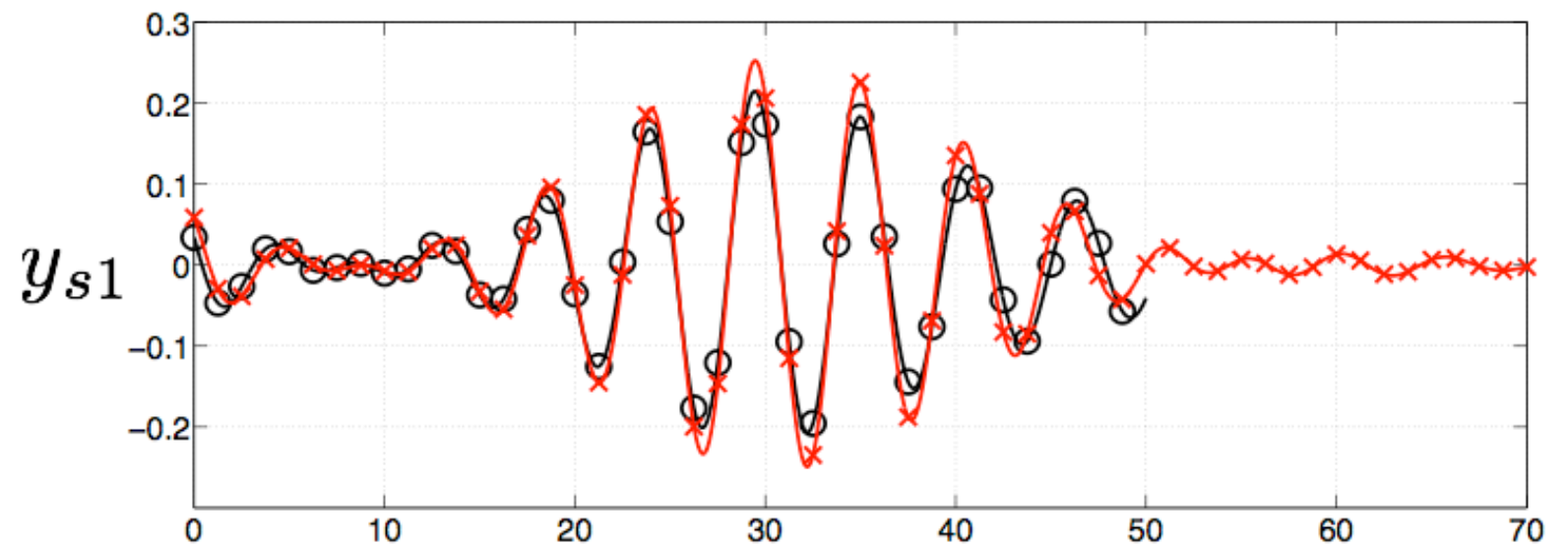
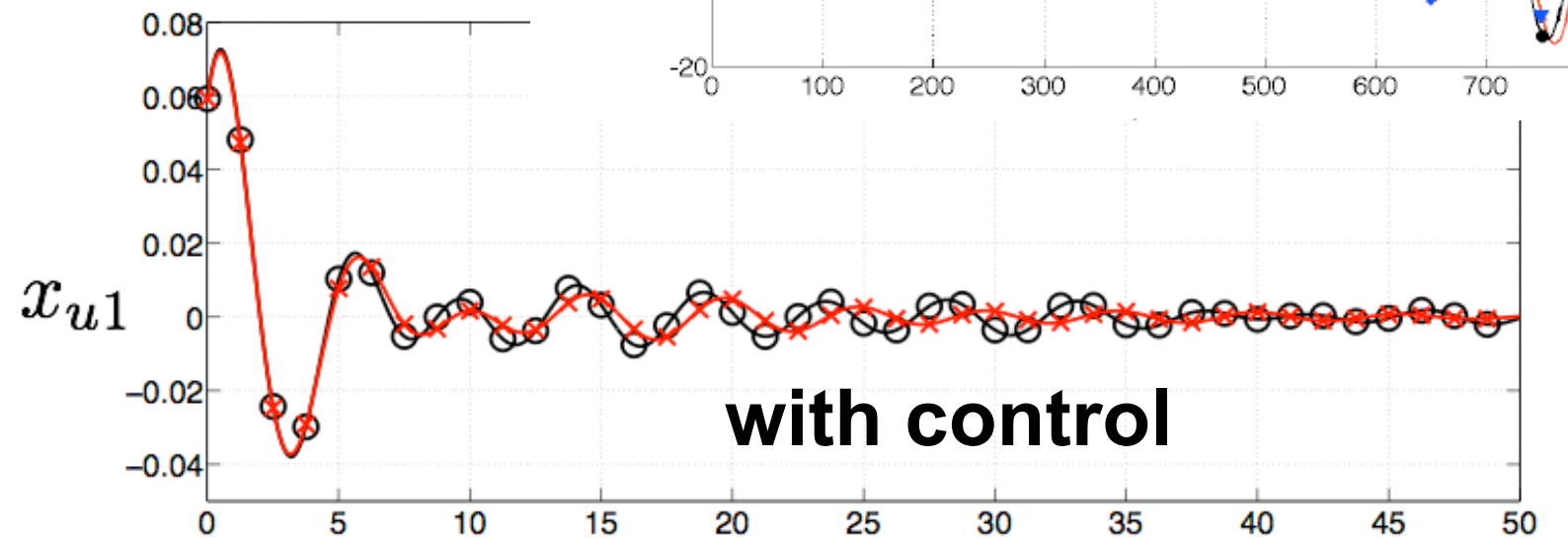


without control



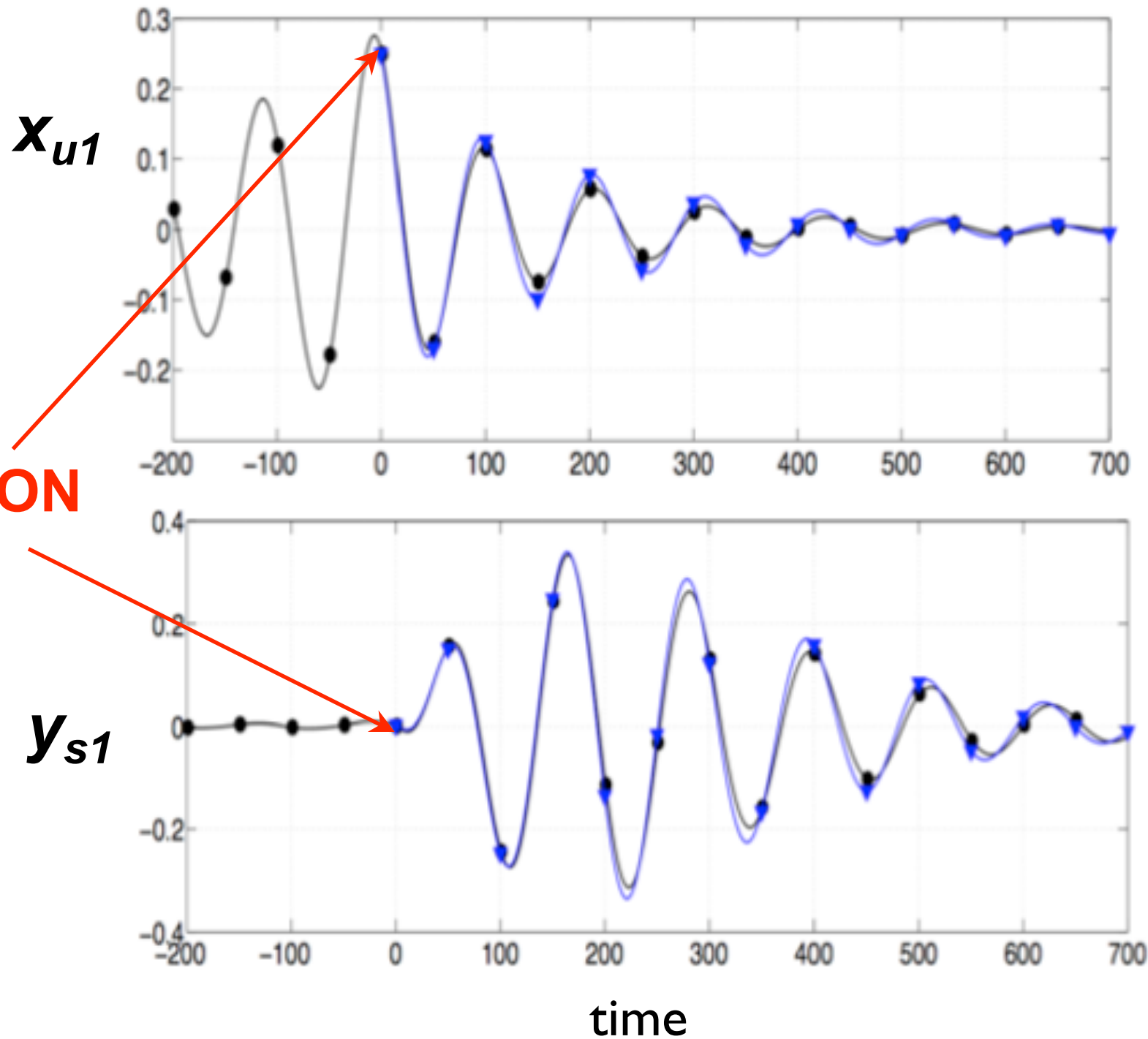
- Control based on a 10-mode model
- Gain K using LQR

with control

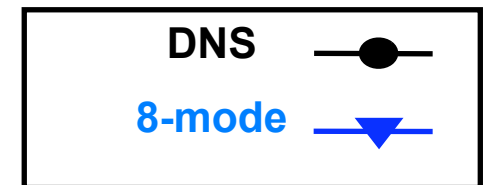


Control in full nonlinear system: close to steady state

Results of an 8-mode model



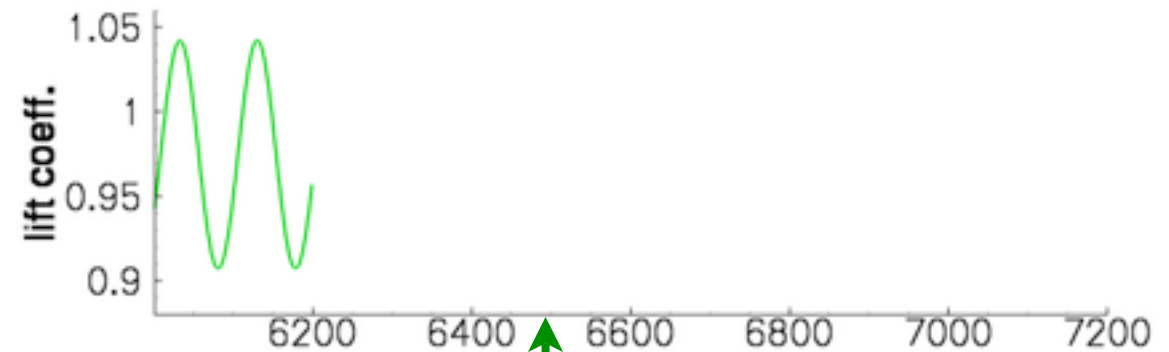
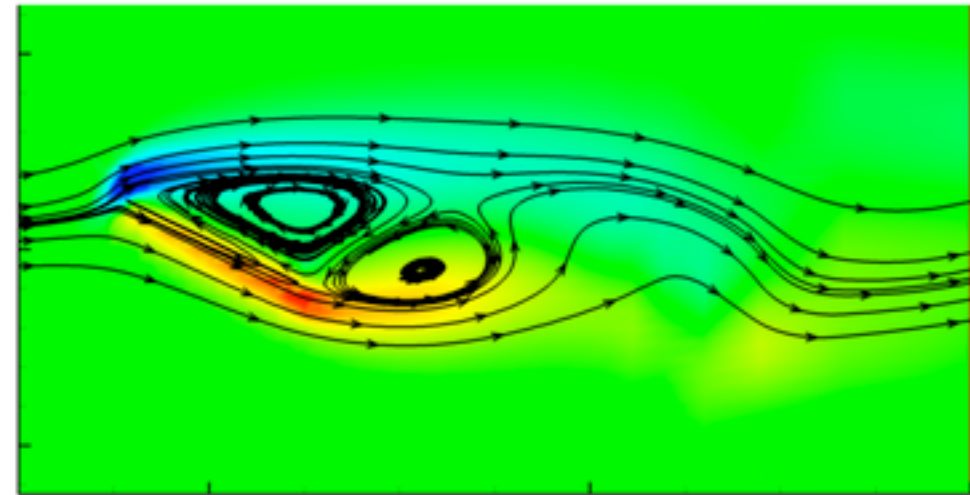
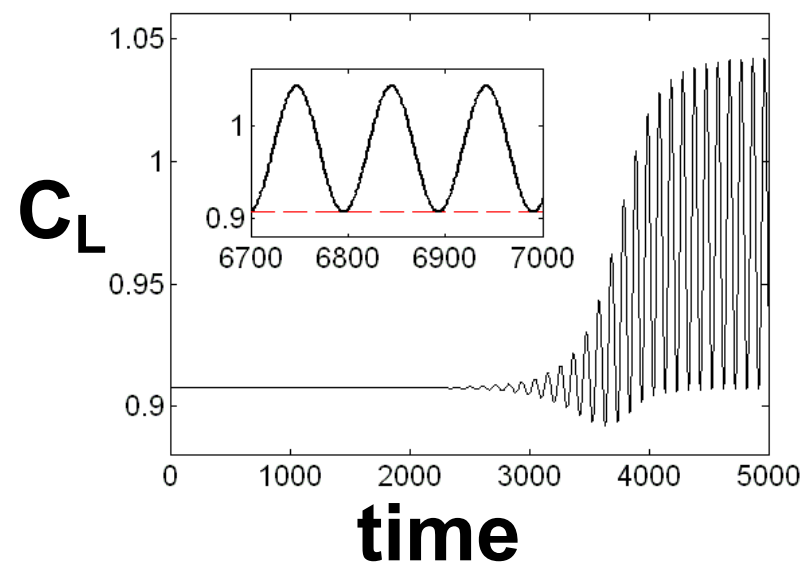
Control ON



Feedback stabilization at $AoA=25$

- Full state feedback
- Large domain of attraction even in the full NL system
- Controller suppresses the vortex shedding

No control

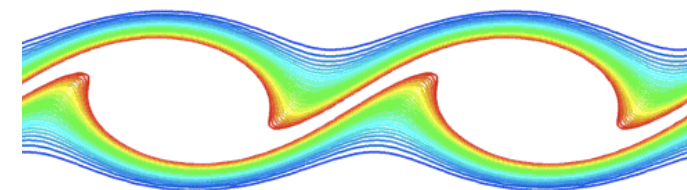
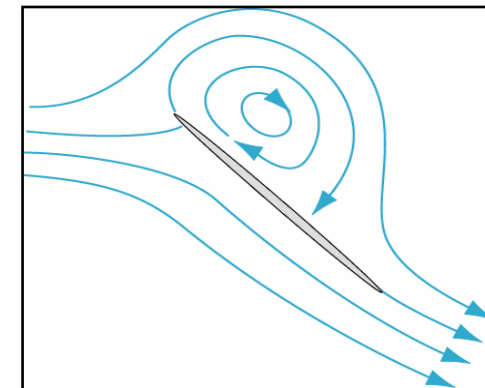
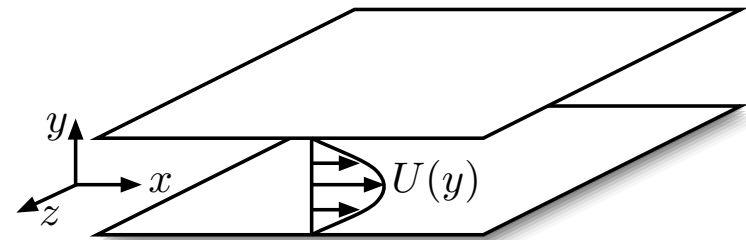


Control on



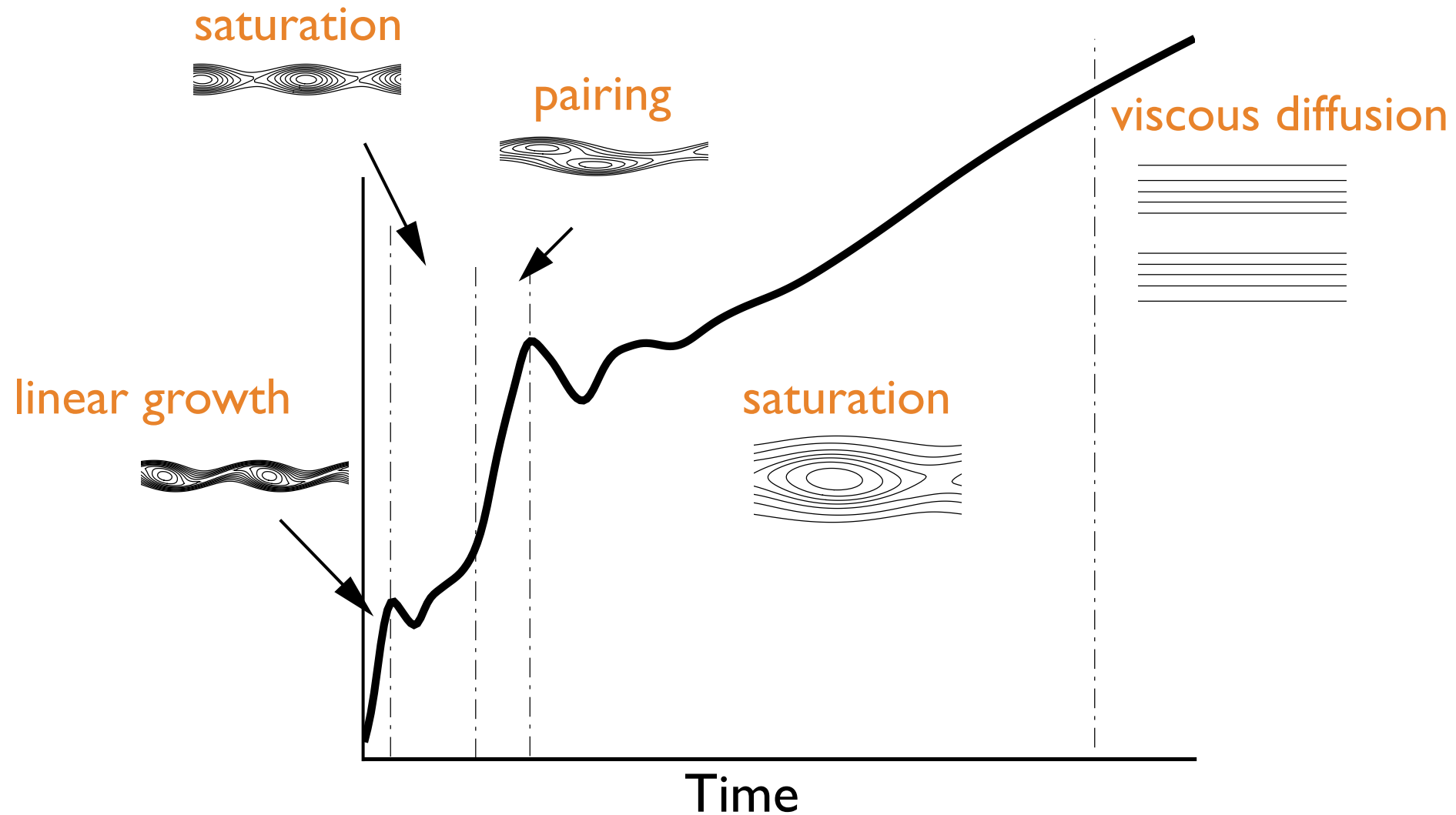
Outline

- Reduced-order models: POD and balanced truncation
 - Importance of inner product for Galerkin projection
 - Balanced truncation
 - Method of snapshots
- Applications
 - Linearized channel flow
 - Separating flow past an airfoil
- Dynamically scaling POD modes
 - Free shear layer
 - Scaled basis functions
 - Template fitting
 - Equations for the shear layer thickness



Modeling free shear layers

- Evolution history of thickness for temporal shear layer (spatially periodic):



- Model initial linear growth, saturation, pairing, and eventual viscous diffusion

[Mingjun Wei, CW Rowley, JFM, to appear, 2008]



Methodology

- Scale POD modes dynamically in y direction to account for shear layer spreading
- Scaling invariants:
 - divergence of velocity field
 - inner product
- Key idea: template fitting
- Main result: an equation for the shear layer spreading rate:
 - as usual, also get equations for time coefficients of POD modes



Scaling basis functions

- Write solution in scaled reference frame

$$\mathbf{q} = (u, v)$$

$$\mathbf{q}(x, y, t) = G(g)\tilde{\mathbf{q}}(x, g(t)y, t)$$

- Choose $G(g) = \begin{bmatrix} 1 & 0 \\ 0 & 1/g \end{bmatrix}$: $\text{div } \mathbf{q} = \text{div } \tilde{\mathbf{q}}$
- Expand scaled variable $\tilde{\mathbf{q}}$ in terms of POD modes

$$\tilde{\mathbf{q}}(x, y, t) = \mathbf{u}_0(y) + \sum_{j=1}^n a_j(t)\varphi_j(x, y)$$

- Advantage of the scaling: capture similar-looking structures as shear layer spreads
- Advantage of divergence-invariant mapping: automatically satisfy continuity equation; simplify pressure term



Template fitting

- How do we choose the scaling $g(t)$?
 - Choose $g(t)$ so that $\tilde{\mathbf{q}}(x, y, t)$ lines up best with a preselected **template** (here, the base flow):

$$\frac{d}{ds} \Big|_{s=0} \|\tilde{\mathbf{q}}(x, y, t) - \mathbf{u}_0(x, h(s)y)\|^2 = 0$$

for any curve $h(s) > 0$ with $h(0) = 1$

- This means the scaled solution $\tilde{\mathbf{q}}(x, y, t)$ satisfies

$$\left\langle y \frac{\partial \mathbf{u}_0}{\partial y}, \tilde{\mathbf{q}} - \mathbf{u}_0 \right\rangle = 0$$

- Geometrically, the set of all “properly scaled” functions $\tilde{\mathbf{q}}$ is an affine space through \mathbf{u}_0 and orthogonal to $y \partial_y \mathbf{u}_0$
- This enables one to write dynamics for how the thickness

$g(t)$ evolves

$$\frac{\dot{g}}{g} = \frac{\langle f_g^1(\tilde{u}), y \partial_y u_0 \rangle}{\langle y \partial_y \tilde{u}, y \partial_y u_0 \rangle}$$



Equation for evolution of the thickness

- How does $g(t)$ evolve in time?
 - We have a constraint ($\tilde{\mathbf{q}}(x, y, t)$ lines up best with template \mathbf{u}_0):

$$\left\langle y \frac{\partial \mathbf{u}_0}{\partial y}, \tilde{\mathbf{q}} - \mathbf{u}_0 \right\rangle = 0$$

- Differentiate:

$$\left\langle y \frac{\partial \mathbf{u}_0}{\partial y}, \frac{\partial \tilde{\mathbf{q}}}{\partial t} \right\rangle = 0$$

- Use equations of motion

$$\frac{\partial \tilde{\mathbf{q}}}{\partial t} = f_g(\tilde{\mathbf{q}}) - \frac{\dot{g}}{g} y \frac{\partial \tilde{\mathbf{q}}}{\partial y} - G(1/g) \dot{G}(g, \dot{g}) \tilde{\mathbf{q}}(x, y, t)$$

- This gives an equation for g :

$$\frac{\dot{g}}{g} = \frac{\langle f_g^1(\tilde{\mathbf{u}}), y \partial_y u_0 \rangle}{\langle y \partial_y \tilde{\mathbf{u}}, y \partial_y u_0 \rangle}$$



Results

- Base flow with small perturbation
 - Base flow: $u_0 = U_c \operatorname{erfc}(\eta), \quad \eta = \frac{-y}{2g} \sqrt{\frac{\operatorname{Re}}{t_0}}$
 - Perturbation is along the unstable eigenfunction of the linearized problem
- Consider three separate cases
 - Self-similar solution (no perturbation)
 - [Vortex roll-up transient (perturbation with $k=1$)]
 - Vortex pairing transient (perturbation with $k=2$):
 - vortex roll-up
 - pairing
 - $k=1$ mode arises through pairing

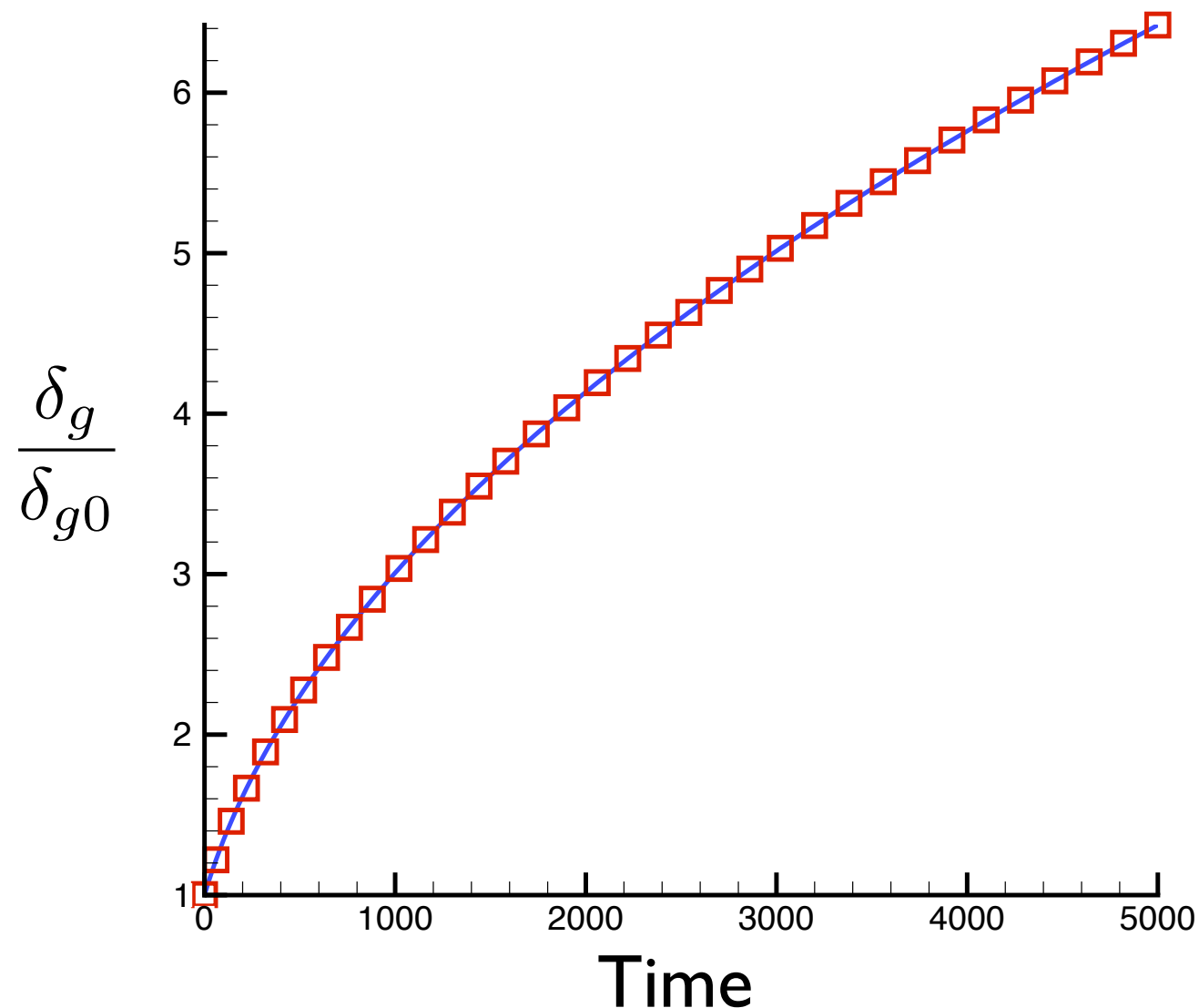


Model results: $k=0$

- Only one equation left for g :

$$\dot{g} = \frac{1}{\text{Re } n_0} \frac{d_0}{g^3} \implies \dot{g} = -\frac{g^3}{2t_0} \implies g(t) = \sqrt{\frac{t_0}{t}}$$

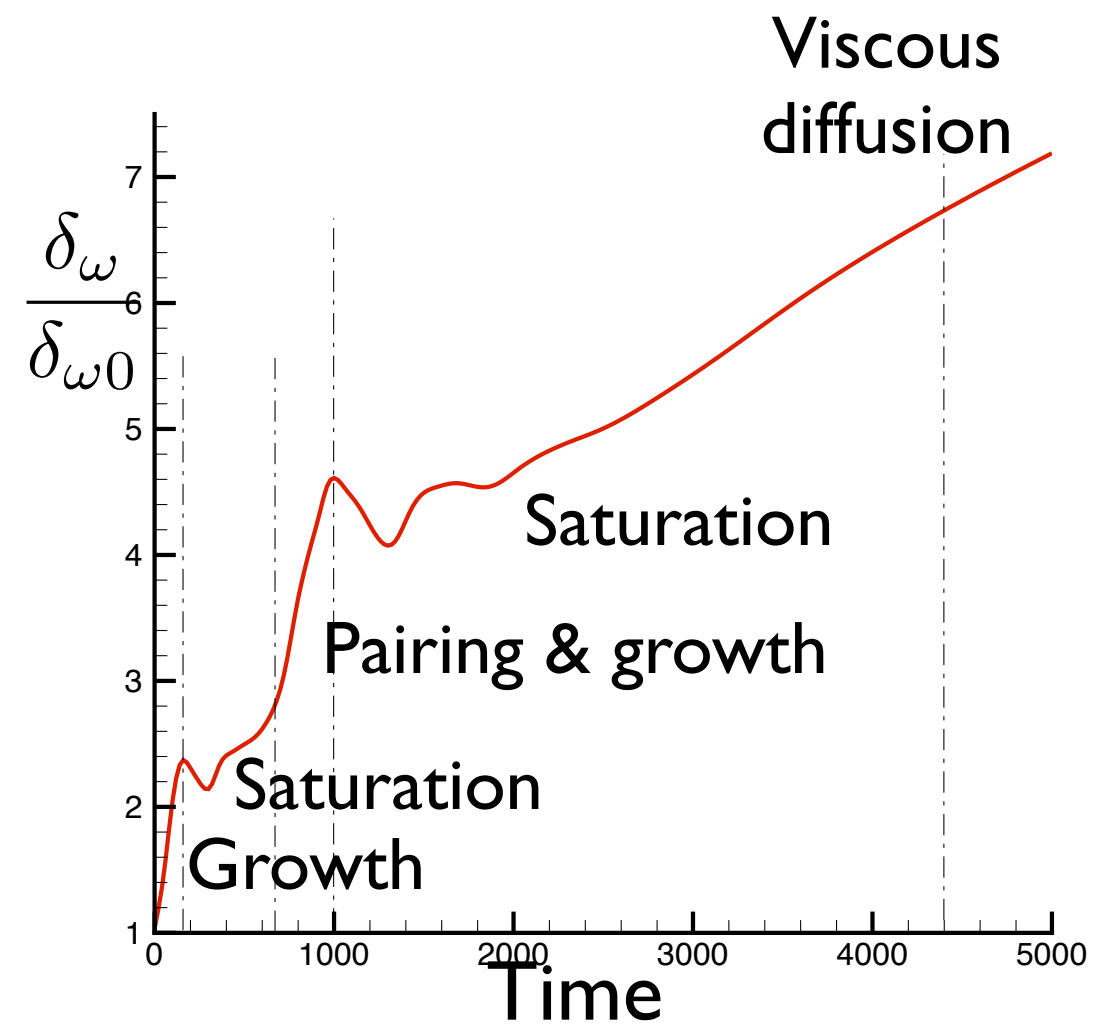
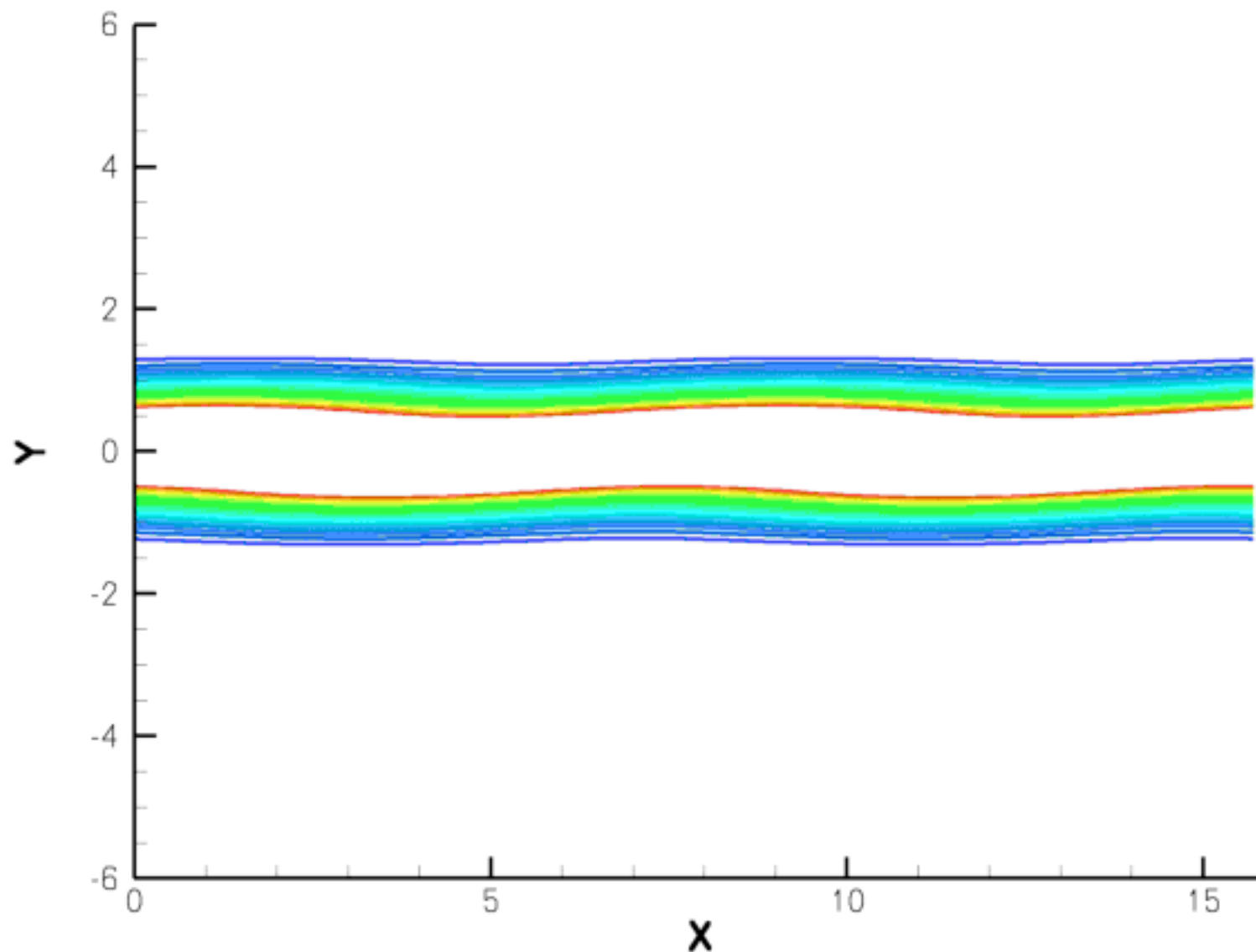
- Recovers exact theoretical growth rate for Stokes problem:



Movie of DNS

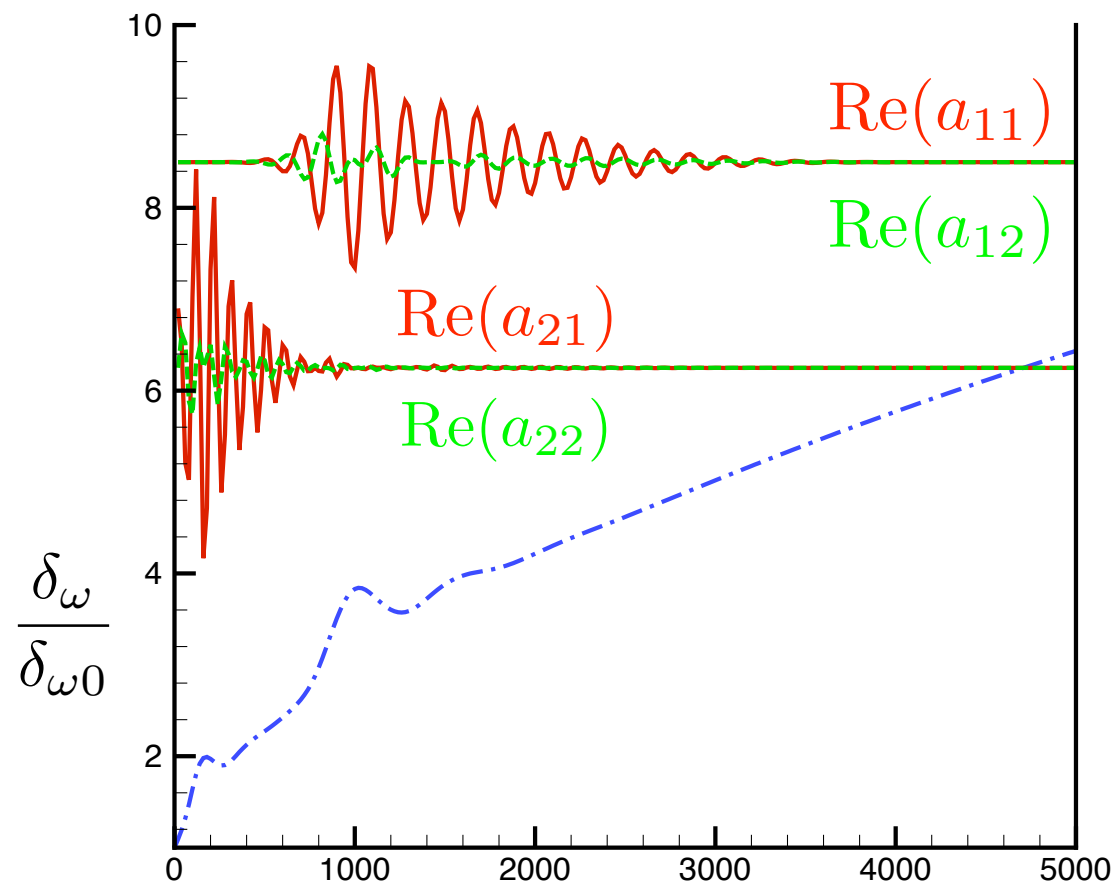
- Vortex pairing (initial condition with $k=2$) $Re = 200$

$k = 2$ simulation

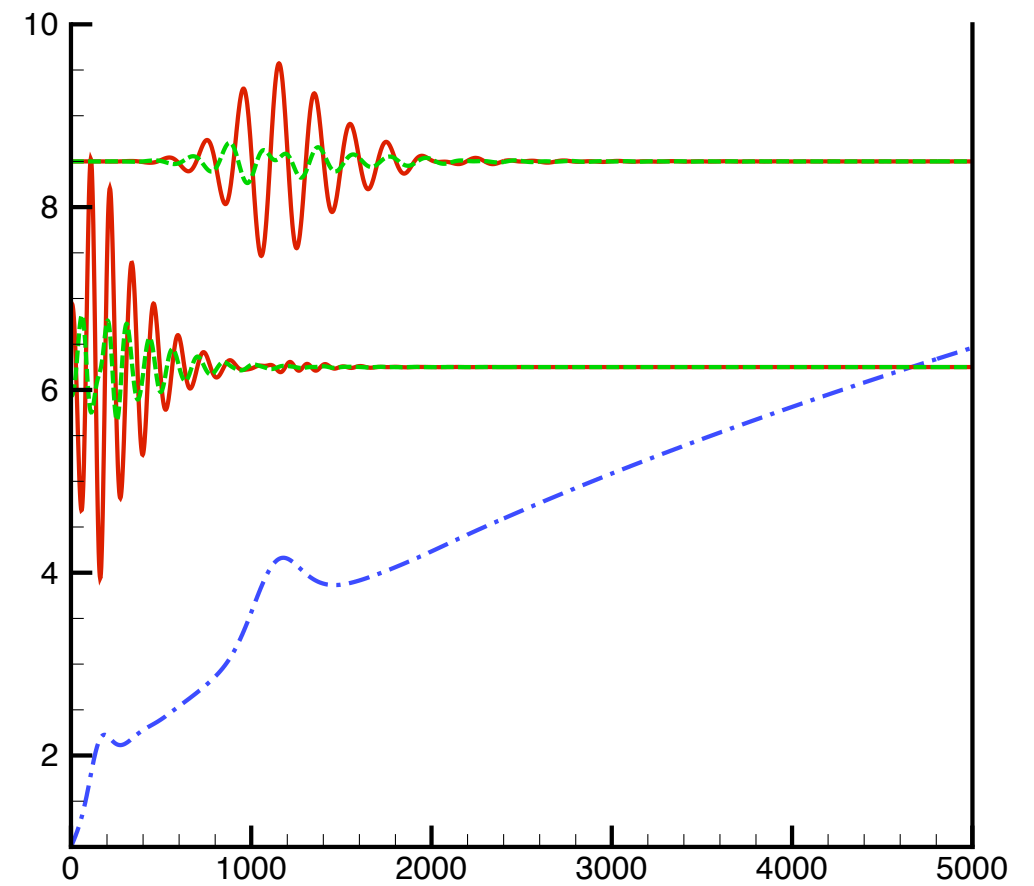


Model results: k=2

- Thickness and amplitude of POD modes for k=2 initial condition: **projection of full simulation**



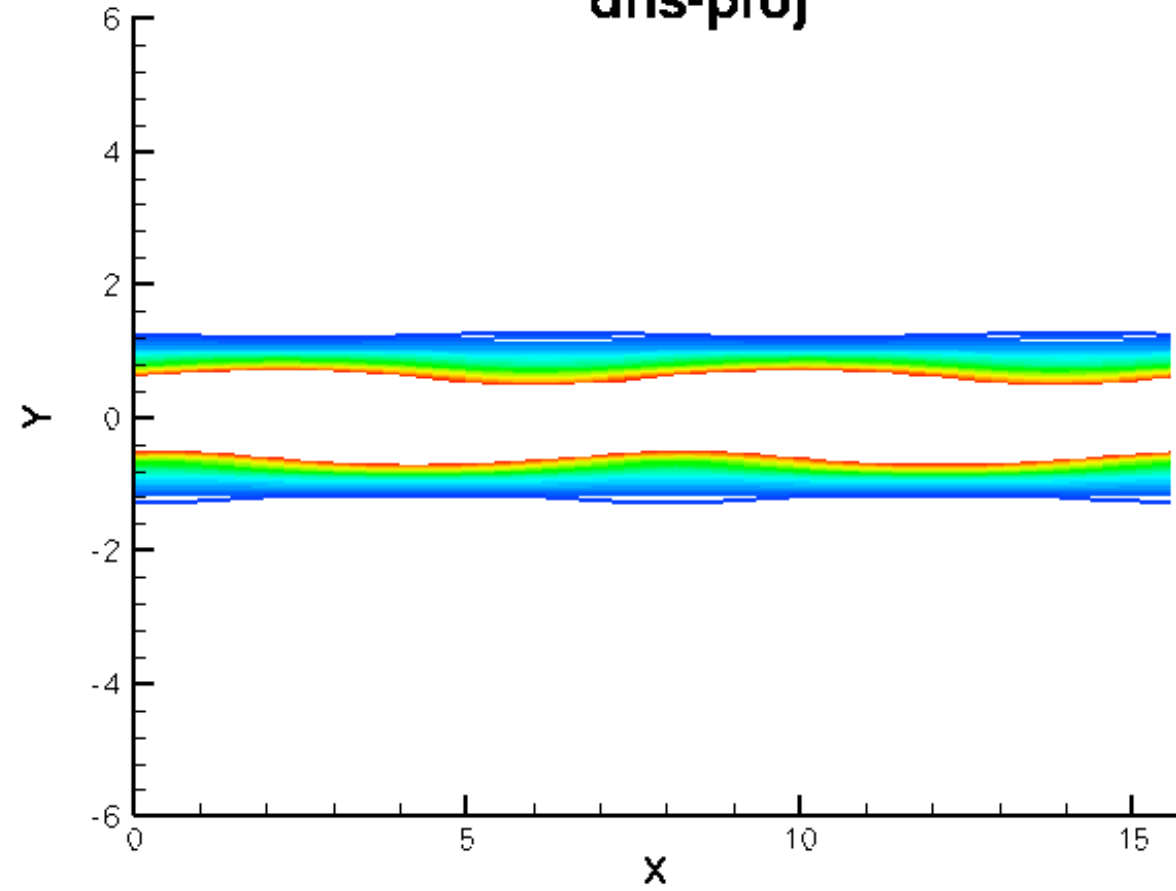
- Thickness and amplitude of POD modes for k=2 initial condition: **low-dimensional model**



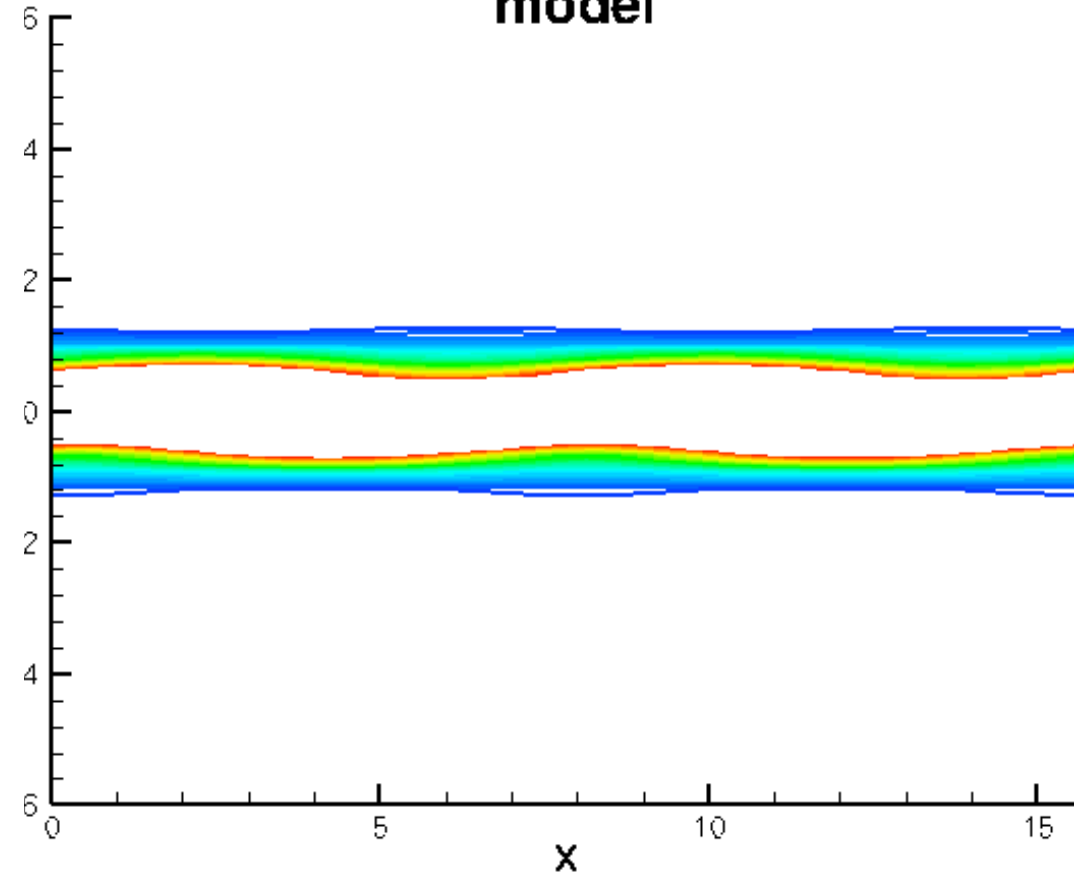
DNS v.s. Model

- Comparison of simulation and model results

dns-proj



model



Summary

- Approximate balanced truncation
 - Approximates exact balanced truncation to as high accuracy as desired, using snapshots from linearized and adjoint simulations
 - Computational cost similar to POD, once snapshots computed
 - For a given number of modes, transients and frequency response much more accurately captured than POD models of same order
 - Extension of basic approach to model unstable linear systems
 - Feedback controllers designed from these models perform well, even on full-order, nonlinear systems
 - Extensions to (weakly) nonlinear systems straightforward
- Dynamically scaled POD modes
 - For systems with self-similar behavior, dynamic scaling decreases number of modes required
 - Temporal shear layer dynamics modeled with 4 complex modes, including linear growth, saturation, pairing, and viscous diffusion

